■ Reaction Mechanisms |*Hot Paper*|

σ-Insertive Mechanism versus Concerted Non-insertive Mechanism in the Intramolecular Hydroamination of Aminoalkenes Catalyzed by Phenoxyamine Magnesium Complexes: A Synthetic and Computational Study

Xiaoming Zhang,[a] Sven Tobisch,*[b] and Kai C. Hultzsch*[a, c]

Abstract: The phenoxyamine magnesium complexes [{ONN}MgCH₂Ph] (**4a**: {ONN} = 2,4-*t*Bu₂-6-(CH₂NMeCH₂CH₂-NMe₂)C₆H₂O⁻; **4b**: {ONN} = 4-*t*Bu-2-(CH₂NMeCH₂CH₂NMe₂)-6-(SiPh₃)C₆H₂O⁻) have been prepared and investigated with respect to their catalytic activity in the intramolecular hydroamination of aminoalkenes. The sterically more shielded triphenylsilyl-substituted complex **4b** exhibits better thermal stability and higher catalytic activity. Kinetic investigations using complex **4b** in the cyclisation of 1-allylcyclohexyl)methylamine (**5b**), respectively, 2,2-dimethylpent-4-en-1-amine (**5c**), reveal a first-order rate dependence on substrate and catalyst concentration. A significant primary kinetic isotope effect of 3.9 ± 0.2 in the cyclisation of **5b** suggests significant N–H bond disruption in the rate-determining transition state. The stoichiometric reaction of **4b** with **5c** revealed that at least two substrate molecules are required per magnesium centre to facilitate cyclisation. The reaction mechanism was further scrutinized computationally by examination of two rivalling mechanistic pathways. One scenario involves a coordinated amine molecule assisting in a concerted non-insertive N–C ring closure with concurrent amino proton transfer from the amine onto the olefin, effectively combining the insertion and protonolysis step to a single step. The alternative mechanistic scenario involves a reversible olefin insertion step followed by rate-determining protonolysis. DFT reveals that a proton-assisted concerted N–C/C–H bond-forming pathway is energetically prohibitive in comparison to the kinetically less demanding σ-insertive pathway ($\Delta\Delta G^{\ddagger} = 5.6$ kcal mol⁻¹). Thus, the σ-insertive pathway is likely traversed exclusively. The DFT predicted total barrier of 23.1 kcal mol⁻¹ (relative to the {ONN}Mg pyrrolide catalyst resting state) for magnesium–alkyl bond aminolysis matches the experimentally determined Eyring parameter ($\Delta G^{\ddagger} = 24.1(\pm 0.6)$ kcal mol⁻¹ (298 K)) gratifyingly well.

Introduction

Nitrogen-containing compounds represent valuable and industrially important bulk chemicals, specialty chemicals and pharmaceuticals.[1] The hydroamination reaction[2] offers facile access to amines, enamines and imines in a waste-free, highly atom-efficient and green manner. Research efforts have focused primarily on the development of transition metal-based catalyst systems (early transition metals of Group 3–5 including the lanthanides,[3–6] actinides,[7] and late transition metals of

Group 8–12[8]) in the last two decades. Main group metal-based catalysts have been studied more intensely only recently. For example, alkali metal-based hydroamination catalysts have been known since the 1950s,[9] but more detailed studies have only begun to emerge in recent years.[10] Alkaline-earth metal complexes[11] are also quite active catalysts for the hydroamination of alkenes[12,13] thanks to the similarity between the chemistry of alkaline-earth metals and that of the rare-earth metals. Unfortunately, alkaline-earth metal complexes are prone to facile Schlenk-type ligand redistributions[11,14] that have hampered the development of chiral alkaline-earth metal hydroamination catalysts for enantioselective hydroamination reactions.[15] However, we have recently developed phenoxyamine {ONN} magnesium complexes (Figure 1)[13,16,17] that resist ligand redistribution and a chiral catalyst, complex **2**, which achieved enantioselectivities of up to 93% *ee* in the intramolecular hydroamination of aminoalkenes.[13b]

The alkaline-earth metal-catalysed hydroamination reaction is generally believed to proceed in a similar manner as has been proposed for rare-earth metal-based catalysts.[3c,18] A metal amide species **A** undergoes migratory olefin insertion, followed by protonolysis of the metal alkyl intermediate **B** to

[a] *Dr. X. Zhang, Prof. Dr. K. C. Hultzsch*
Department of Chemistry and Chemical Biology, Rutgers
The State University of New Jersey, 610 Taylor Road
Piscataway, NJ 08854-8087 (USA)

[b] *Dr. S. Tobisch*
University of St. Andrews, School of Chemistry
Purdie Building, North Haugh, St. Andrews, KY16 9ST (UK)
E-mail: st40@st-andrews.ac.uk

[c] *Prof. Dr. K. C. Hultzsch*
Present address: University of Vienna, Faculty of Chemistry
Institute of Chemical Catalysis, Währinger Strasse 38, 1090 Vienna (Austria)
E-mail: kai.hultzsch@univie.ac.at

🖥 Supporting information for this article is available on the WWW under
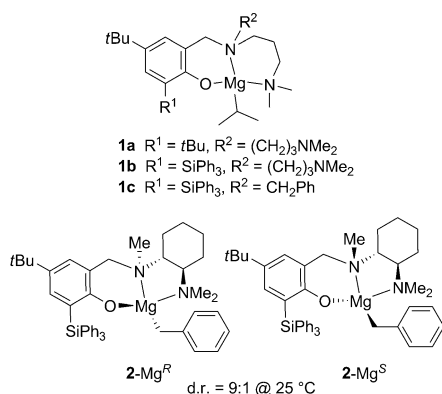http://dx.doi.org/10.1002/chem.201406468.

Figure 1. Previously studied phenoxyamine {ONN} magnesium hydroamination catalysts.[13, 17]

regenerate the catalytically active metal amide species **A** (Scheme 1). Rare-earth metal-based catalyst systems are commonly thought to involve a rate-determining olefin insertion step and fast protonolysis, resulting in zeroth order rate dependency on substrate concentration. The relative rate of the two steps is less clear for catalysts based on alkaline-earth metals, because these catalysts predominantly,[12f, m–o, w, 13b] with a few exceptions,[13a] display a first-order rate dependence on substrate concentration, which is contradictory to a fast protonolysis step.
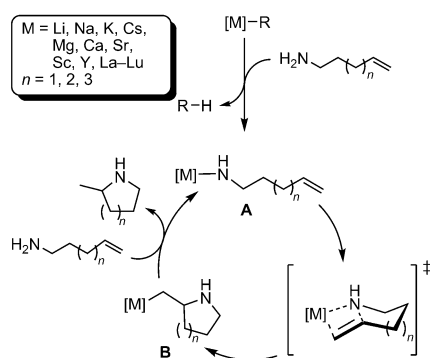
Scheme 1. Postulated general mechanism for hydroamination/cyclisation of aminoalkenes catalysed by alkali, alkaline-earth and rare-earth metals.

However, the observation of a significant primary kinetic isotope effect[3c, w, z, 4d, 5s–v, 12m–o, w, 13] and isotopic perturbation of stereoselectivity[3c, w, 5v] in a number of catalyst systems based on various metals are indicative of significant N–H bond disruption in the transition state of the stereo- and rate-determining alkene insertion step. A plausible explanation for these contradictory observations involves partial proton transfer from a coordinated amine to the terminal olefin carbon of the aminoalkene substrate in the ring-closing transition state (Scheme 2).[3c] Similar concerted reaction mechanisms have been proposed for a number of alkaline-earth[12m, n] and Group 4[5t–v] metal catalysts. A DFT study[19] performed on a bis(ureate)-zirconium metal catalyst system[5u] has indeed confirmed this proposal, while a study on a tris(oxazolinyl)phenylborate mag-
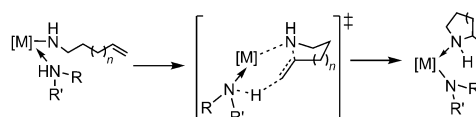
Scheme 2. Proposal for a concerted non-insertive N–C ring closure with concurrent amino proton transfer onto the olefin in the hydroamination/cyclisation (RR′NH = substrate or hydroamination product).

nesium[20] and a cyclopentadienyl-bis(oxazolinyl)borate yttrium[18h] catalyst system indicate that the reaction proceeds via a reversible migratory insertion step followed by rate-determining protonolysis.

In the present study we will scrutinize two rivalling mechanistic pathways for the intramolecular hydroamination of aminoalkenes utilizing novel phenoxyamine {ONN} magnesium complexes. One working hypothesis was that a coordinated amine molecule could assist in a concerted non-insertive N–C ring closure with concurrent amino proton transfer from the amine onto the olefin (Scheme 2), effectively combining the insertion and protonolysis step to a single step. An alternative scenario implies a reversible olefin insertion step and a rate-determining protonolysis step (Scheme 3).
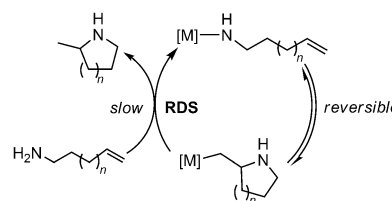

Scheme 3. Proposal for an alternative mechanistic scenario with reversible olefin insertion and rate-determining protonolysis.

Results and Discussion

Synthesis and characterization of model systems

In accordance with a previous study on a chiral phenoxydiamine magnesium catalyst,[13b] the related achiral magnesium complexes **4a** and **4b** incorporating an ethylenediamine sidearm can be most conveniently prepared via alkane elimination by treating the appropriate phenoldiamine proligands **3a**, respectively, **3b**, with Mg(CH₂Ph)₂(THF)₂ in a 1-to-1 molar ratio at room temperature (Scheme 4). The di-tert-butyl-substituted complex **4a** proved to be rather unstable and attempts to isolate complex **4a** in solid form failed, due to formation of a ligand redistribution product upon removal of solvent. Therefore, complex **4a** was generally prepared in situ and was used directly for catalytic experiments. Complex **4b** was obtained as a white foam which is partially soluble in hexanes. Unfortunately, all efforts to obtain X-ray quality crystals have been unsuccessful so far. Complex **4b** is stable at room temperature in the solid state for several hours; however, slow decomposition was observed over 3 days.
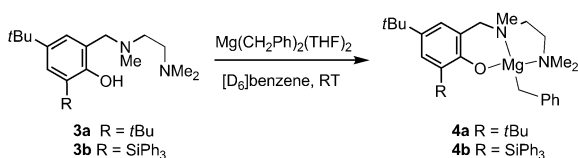
Scheme 4. Synthesis of phenoxyamine {ONN} magnesium complexes.

The ^{1}H NMR spectrum of complex **4b** exhibits fluxional be-haviour for the ethylenediamine sidearm similar to that ob-served previously for the phenoxytriamine complex **1b**.[13a]

Catalytic hydroaminations

The catalytic activity of complexes **4a** and **4b** was studied in the intramolecular hydroamination of a range of aminoalkene substrates and can be compared to previously investigated phenoxyamine magnesium catalysts (Table 1).

The sterically less hindered *tert*-butyl-substituted catalyst **4a** displays significantly lower activity than the sterically more hin-dered triphenylsilyl-substituted catalyst **4b** (Table 1, entry 6 vs. 7 and entry 12 vs. 13). This observation is in agreement to find-ings of a previous study that compared the activity of com-plexes **1a** and **1b**.[13a] The activity of complex **4a** seems to be comparable to complex **1a**, whereas the activity of **4b** falls be-tween the phenoxytriamine complex **1b** and the chiral com-plex **2**. Thus, **4b** facilitates smooth cyclisation of *gem*-dialkyl and *gem*-diphenyl substituted aminopentenes **5a–c** as well as substrates **5d** and **5e** containing a vinylic phenyl group at room temperature (Table 1, entries 1, 7, 13, 18, and 23). The cyclisation of the aminohexene derivative **5f** also proceeded at room temperature, but required 3 days to reach completion (Table 1, entry 28). Only the cyclisation of the N-benzylated substrate **5g** required heating of the reaction mixture (Table 1, entry 33). Therefore, further kinetic and mechanistic studies were performed with the more active and more stable catalyst **4b**.

Mechanistic and kinetic studies

A kinetic investigation utilizing complex **4b** in the hydroamina-tion/cyclisation of substrate **5b** revealed a first-order rate de-pendence on substrate concentration (Figure 2 and Figure 3), as well as a first order rate dependence on catalyst concentra-tion (Figure 4). The cyclisation of **5b** with the sterically less de-manding, *tert*-butyl-substituted catalyst **4a** also proceeds with a first-order rate dependence on substrate concentration (Fig-ure S1 in the Supporting Information). These observations are in agreement with the catalytic behaviour of complex **1a** and **2**; however, they contrast the behaviour of complex **1b**, which exhibits zeroth order rate dependence on substrate concentra-tion.[13]

The cyclisation of the N-deutero substrate **[D₂]5b** with com-plex **4b** exhibited a significant primary kinetic isotope effect (KIE) of 3.9 ± 0.2 (Figure 5), in agreement with previous obser-vations for complexes **1b** and **2**.[13] Similar KIE's have been also
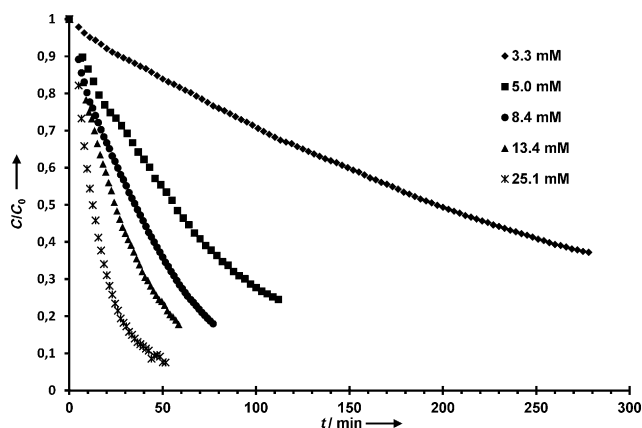

Figure 2. Time dependence of substrate concentration in the hydroamina-tion/cyclisation of (1-allylcyclohexyl)methylamine (**5b**, normalized to $C_0 = 0.167 \text{ mol L}^{-1}$) in [D₆]benzene at 25 °C using varying concentrations of **4b**. The error of measurement for the data points is estimated to be $\pm 5\%$ based on the accuracy of integrating signals in a ^{1}H NMR spectrum (error bars are omitted for clarity).
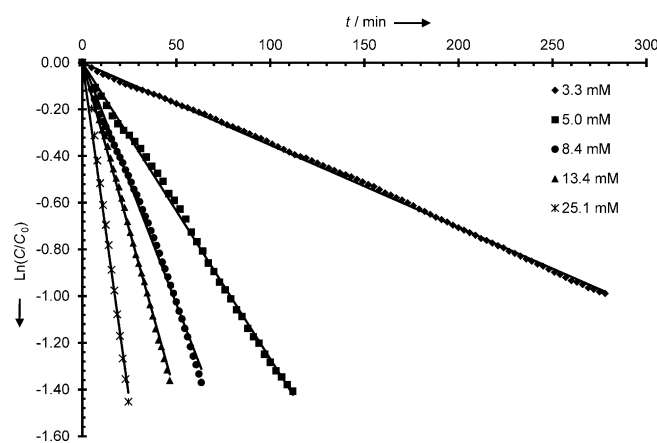

Figure 3. Logarithmic plot of normalized substrate concentration versus time for the hydroamination/cyclisation of (1-allylcyclohexyl)methylamine (**5b**, $C_0 = 0.167 \text{ mol L}^{-1}$) in [D₆]benzene at 25 °C using varying concentrations of **4b**.
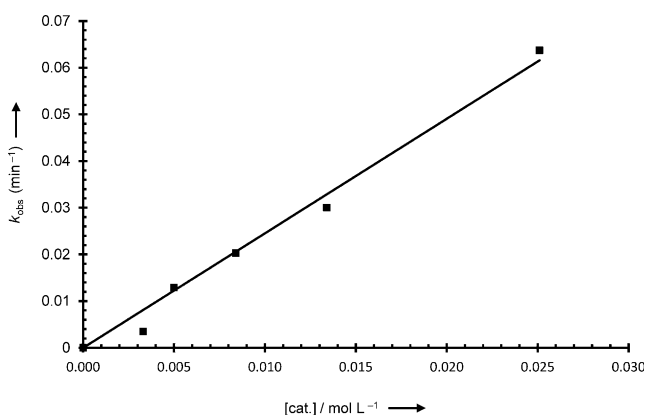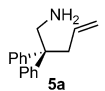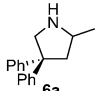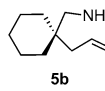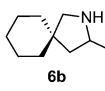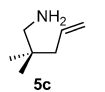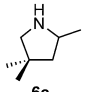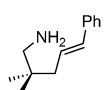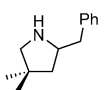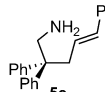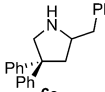

Figure 4. Dependence of observed rate on catalyst concentration for the hydroamination/cyclisation of (1-allylcyclohexyl)methylamine (**5b**, $C_0 = 0.167 \text{ mol L}^{-1}$) with catalyst **4b** in [D₆]benzene at 25 °C.

Entry	Substrate	Product	Cat. [mol %]	T [°C]	t [h]	Conv. [%]	Ref.
	5a	**6a**					
1			**4b** (5)	22	3	99	this work
2			**1a** (5)	25	4	99	[13a]
3			**1b** (3)	25	3	99	[13a]
4			**1c** (5)	25	5	98	[13a]
5	**5b**	**6b**	**2** (3)	22	1.5	99	[13b]
6			**4a** (5)	60	4	98	this work
7			**4b** (5)	22	4	98	this work
8			**1a** (10)	25	12	98	[13a]
9			**1b** (5)	25	13	96	[13a]
10			**1c** (5)	25	22	81	[13a]
11	**5c**	**6c**	**2** (5)	22	2	99	[13b]
12			**4a** (5)	110	48	78	this work
13			**4b** (5)	22	36	96	this work
14			**1a** (10)	100	40	98	[13a]
15			**1b** (10)	100	18	98	[13a]
16			**1c** (10)	100	40	48	[13a]
17	**5d**	**6d**	**2** (5)	22	10	97	[13b]
18			**4b** (5)	22	3	99	this work
19			**1a** (10)	100	7	99	[13a]
20			**1b** (10)	100	12	99	[13a]
21			**1c** (10)	100	24	98	[13a]
22	**5e**	**6e**	**2** (5)	22	2	99	[13b]
23			**4b** (5)	22	2	99	this work
24			**1a** (10)	25	2	99	[13a]
25			**1b** (10)	25	1.5	99	[13a]
26			**1c** (10)	25	2	99	[13a]
27	**5f**	**6f**	**2** (5)	22	0.1	99	[13b]
28			**4b** (5)	22	72	96	this work
29			**1a** (10)	60	13	99	[13a]
30			**1b** (10)	60	2.5	99	[13a]
31			**1c** (10)	60	8	99	[13a]
32	**5g**	**6g**	**2** (5)	22	6	98	[13b]
33			**4b** (5)	80	48	95	this work

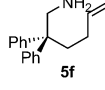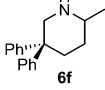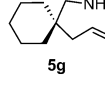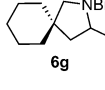Table 1. Hydroamination of aminoalkenes catalysed by magnesium complexes **1 a–c**, **2**, and **4 a,b**.[a]

[a] Reaction conditions: 0.1 mmol substrate, 0.6 mL [D$_6$]benzene, Ar atm.

A kinetic study of the cyclisation of the less reactive *gem*-dimethyl-substituted aminoalkene **5 c** allowed measuring reaction rates in a wider temperature range from 22 to 80 °C (Figure 6). The activation parameters were determined as $\Delta H^{\neq} = 10.5(\pm 0.4)$ kcal mol^{-1} and $\Delta S^{\neq} = -45.7(\pm 1.4)$ cal K^{-1} mol^{-1} from the Eyring plot (Figure 7).

The phenoxyamine magnesium catalyst **4 b** shows signs of product inhibition, as indicated by the observed rate depression when substrate **5 c** is added in two batches (Figure 8). This appears to be in contrast to observations made for complexes **1 b** and **1 c**.[13a] However, this observation is in agreement with previous studies on binaphtholate rare-earth metal complexes[4d] and β-diketiminate calcium amide complexes.[12f]

The stoichiometric reaction of **4 b** with 2,2-dimethylpent-4-en-1-amine (**5 c**) in a 1:1 ratio did not lead to any hydroamination product formation within 5 h at room temperature (Figure 9 a). Subsequent addition of a second equivalent of **5 c** produced 1 equivalent of the hydroamination product **6 c** after 6 h at room temperature (Figure 9 b).

The sharpness of the signals of **6 c** suggests that it is not bound to the magnesium complex, which is corroborated by DFT findings that **6 c** binds less strongly than **5 c** at magnesium in the Mg amido catalyst complex (vide infra, Figure 10). This stoichiometric reaction supports the hypothesis that the cyclisation proceeds only if more than one equivalent of aminoalkene substrate (with respect to the magnesium catalyst) is present in the reaction mixture. Hence, it can be proposed that two substrate molecules are bound to the catalytic metal centre in order for the reaction to proceed. This finding is reminiscent of tris(oxazolinyl)phenylborate magnesium[12n] and cyclopentadienylphosphazene dialkyl rare-

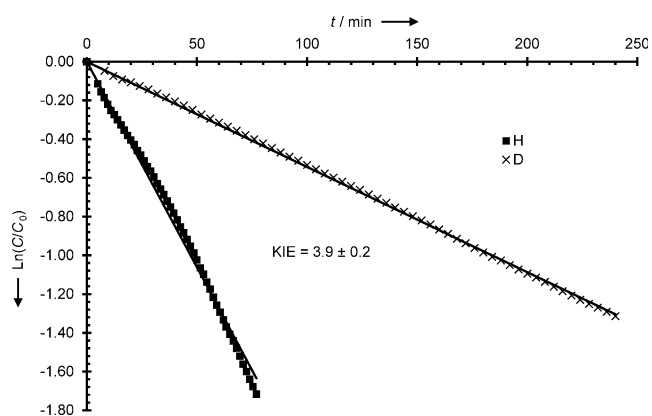observed for alkaline-earth metal,[12m–o,w] rare-earth metal[3c,w,z,4d] and Group 4 metal[3w,5s–v] catalysts.

Figure 5. First order plot for the cyclisation of (1-allylcyclohexyl)methylamine (**5 b**) and [D$_2$](1-allylcyclohexyl)methylamine ([**D$_2$**]**5 b**, $C_0 = 0.167$ mol L^{-1}) in the presence of **4 b** ([cat.] = 8.40 mmol L^{-1}) in [D$_6$]benzene at 25 °C.

Figure 7. Eyring plot for the hydroamination/cyclisation of 2,2-dimethylpent-4-en-1-amine (**5 c**, $C_0 = 0.167$ mol L^{-1}) in [D$_6$]benzene using 5.0 mol % of **4 b** as catalyst.
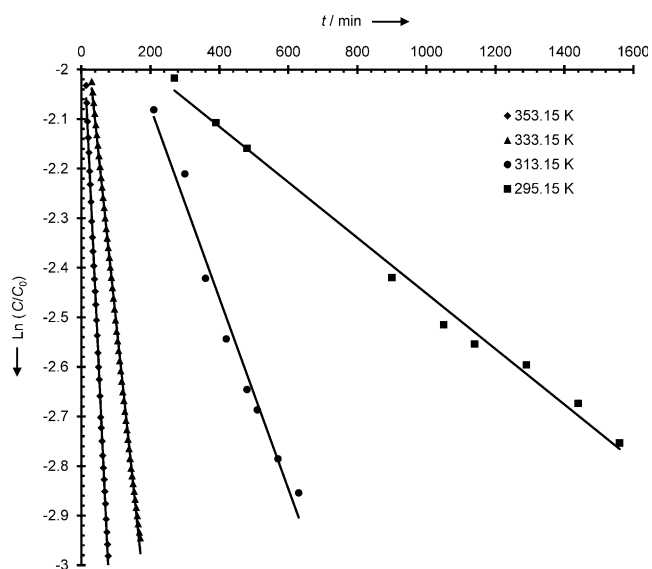

Figure 6. Logarithmic plot of normalized substrate concentration versus time for the hydroamination of 2,2-dimethylpent-4-en-1-amine (**5 c**, $C_0 = 0.167$ mol L^{-1}) in [D$_6$]benzene using 5.0 mol % of **4 b** as catalyst at various temperatures.
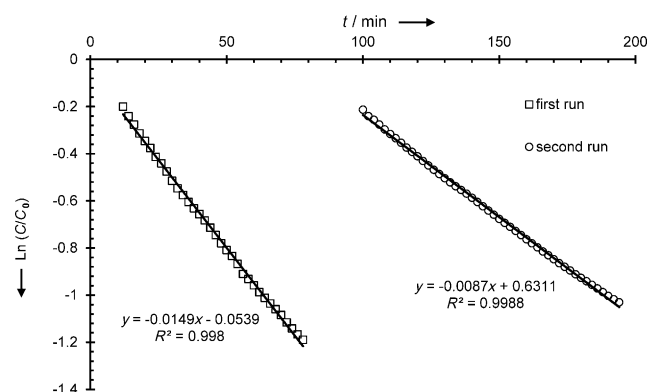
Figure 8. Logarithmic plot of normalized substrate concentration versus time for the hydroamination of 2,2-dimethylpent-4-en-1-amine (**5 c**; first addition: $C_0 = 0.167$ mol L^{-1}) in [D$_6$]benzene using 5.0 mol % of **4 b** ([cat.] = 8.33 mmol L^{-1}) as catalyst at 80 °C. Upon completion of the first run, a second batch of substrate was added. The second run proceeds slower, indicating product inhibition.
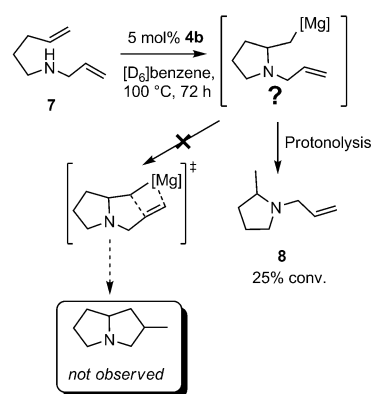
Scheme 5. Attempted hydroamination/carbocyclisation of *N*-allylpent-4-en-1-amine (**7**) with catalyst **4 b**.

earth metal[3z] catalysts that required the addition of more than 2 equiv of aminoalkene substrate before the hydroamination commenced.

A difference between the concerted non-insertive mechanism and the two-step migratory insertion/protonolysis mechanism is the existence of a metal-alkyl intermediate **B** (Scheme 1). The presence of this intermediate for lanthanocene-catalysed hydroamination has been indicated by the successful realization of hydroamination/carbocyclisation sequences.[3e,h,i] In an attempt to prove the intermediacy of species **B** we investigated the reaction of *N*-allylpent-4-en-1-amine (**7**) with catalyst **4 b**. However, the hydroamination product **8** was the only observed product (Scheme 5) and no bicyclic product stemming from a hydroamination/carbocyclisation process was detected. A similar observation was made in a study
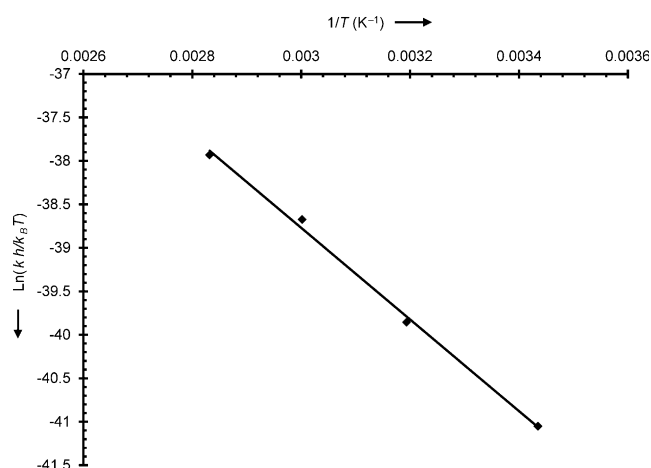
by Hill and co-workers using nacnac calcium hydroamination catalysts.[12f] However, the interpretation with respect to the intermediacy of species **B** in the catalytic process is not unambig-

(a)

(b)
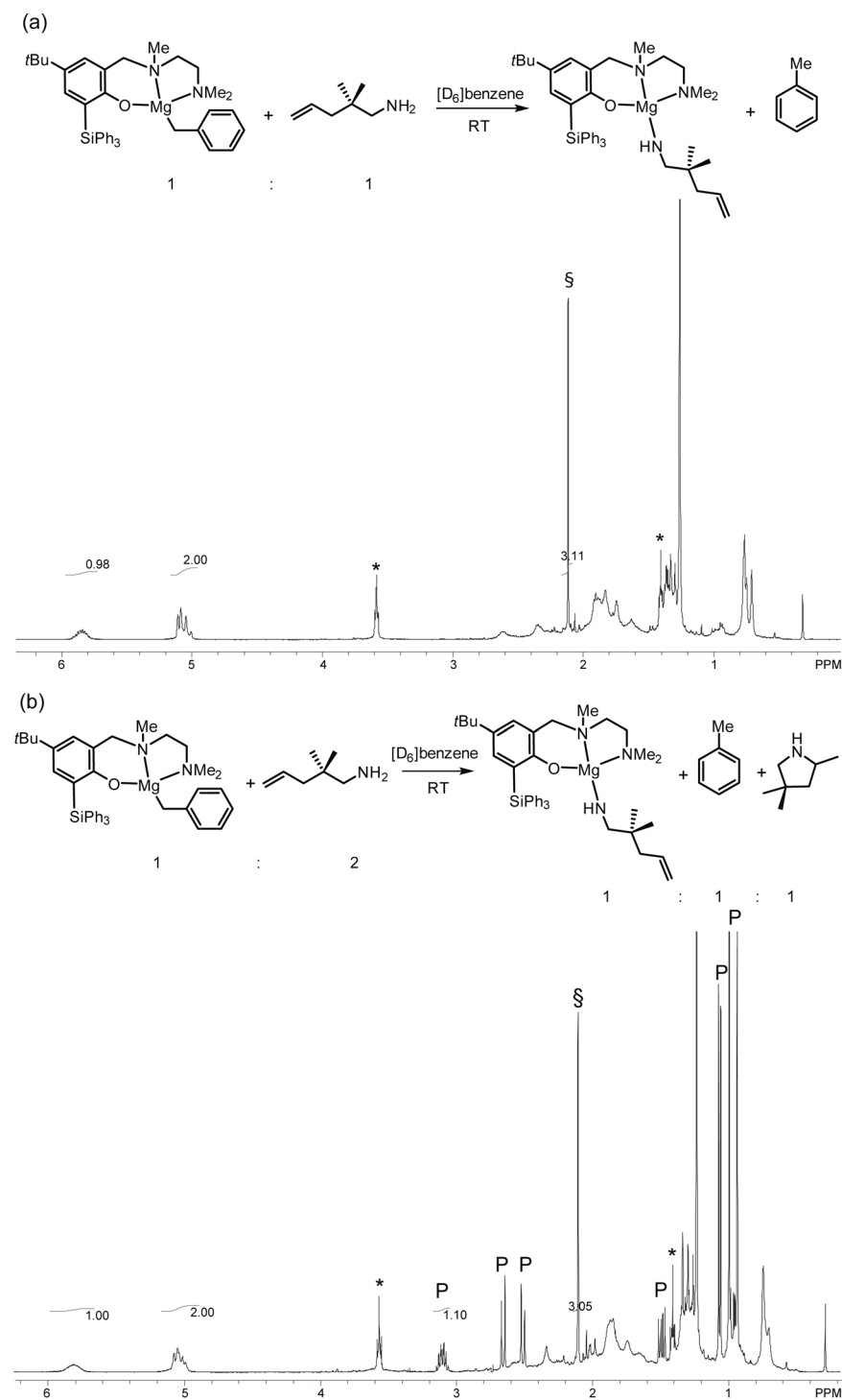
Figure 9. ¹H NMR spectra of stoichiometric reaction of complex **4b** and 2,2-dimethylpent-4-en-1-amine (**5c**) in [D₆]benzene at room temperature. a) Complex **4b/5c** = 1:1, no hydroamination product was observed after 5 h at room temperature. b) Complex **4b/5c** = 1:2, 1 equivalent of hydroamination product **6c** was observed after 6 h at room temperature (§ = toluene formed in reaction of **4b** with **5c**; P = hydroamination product **6c**; * = residual THF).

Computational studies

In order to increase our mechanistic understanding we embarked on a detailed computational analysis of rival mechanistic pathways for cyclisation of the *gem*-dimethyl-substituted aminoalkene **5c** (denoted thereafter as S) into pyrrolidine **6c** (denoted thereafter as P) mediated by compound **4b** (denoted thereafter as **C2**). The DFT method was employed as an established and predictive means to aid mechanistic understanding;[18–20] the computational methodology employed (dispersion-corrected B97-D3 in conjunction with basis sets of triple-ζ quality and a sound treatment of bulk solvent effects, see the Computational Details section for details) simulated authentic reaction conditions adequately and mechanistic analysis is based on Gibbs free-energy profiles. Furthermore, the validity of the computational protocol employed for reliably mapping the energy landscape of alkaline-earth-mediated hydroamination has been substantiated before[18i] and this allowed mechanistic conclusions with substantial predictive value to be drawn. Whilst the presentation herein is restricted exclusively on the most accessible pathways, a complete account of all scrutinised species is given in the Supporting Information.

Catalyst initiation

Effective hydroamination catalysis entails the initial conversion of starting material **C2** (compound **4b**, Scheme 4) into the catalytically competent phenoxy-amine [{ONN}Mg(NHR)] magnesium amidoalkene compound through protonolytic Mg–C alkyl bond cleavage. The initial facile association[21] of one and two aminoalkene (S) molecules is somewhat downhill in free energy, whilst association of a third substrate molecule is seen to be thermodynamically unfavourable. The Mg–C alkyl bond aminolysis commencing from

uous, because one can conclude only that either, 1) species **B** is not an intermediate with a sufficient lifetime to allow the carbocyclisation to proceed, or 2) the activation barrier for the magnesium-catalysed carbocyclisation exceeds the barrier for the other steps in the hydroamination process.

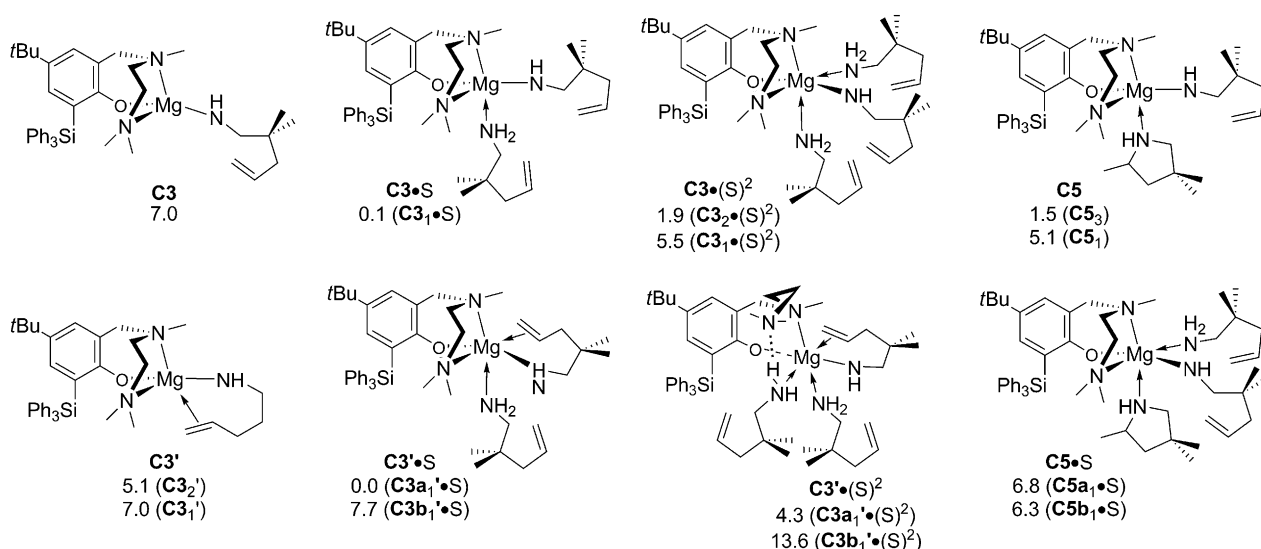**Figure 10.** Amine association at the catalytically relevant [{ONN}Mg(NHR)] compound.[21,23]

substrate adducts $C2 \cdot (S)^n$ evolves through a metathesis-type transition state (TS) that decays thereafter into substrate-free or substrate-adducted forms of the magnesium amido catalyst complex ($C3 \cdot (S)^n$) through facile liberation of toluene. Pathways with one or two substrate molecules involved appear equally feasible.[22] However, the participation of one spectator substrate molecule via $C2 + 2S \rightarrow C3 \cdot S$ stabilises both the TS structure and also the {ONN}Mg amido complex and thus favours this pathway relative to $C2 + S \rightarrow C3$ on both thermodynamic and kinetic grounds (Figure S2 in the Supporting Information). The moderate activation barrier of 13.3 kcal mol^{-1} together with a thermodynamic force of 11.8 kcal mol^{-1} characterises the initial conversion of $C2$ into the magnesium amido catalyst complex as a kinetically easy, essentially irreversible transformation.

The catalytically competent [{ONN}Mg(NHR)] compound

Amine substrate (S) or product (P) molecules can associate in various ways with magnesium at the catalytically competent {ONN}Mg amido compound $C3$ (or A in Scheme 1) to give rise to a multitude of adduct species, all of which are expected to participate in rapid association/dissociation equilibria.[21] The relative stabilities of various located species with one or two adducted amine molecules are collated in Figure 10. Different isomers of a given species are denoted by subscript numbers and also by a or b labelling (see below). A moderately encumbering phenoxyamine {ONN}Mg ligation favours amine association at magnesium, which is capable of accommodating up to two amine molecules. The association pattern for substrate-free and substrate-adducted forms reflects the variation in spatial demands around magnesium. For substrate-free forms, species $C3'$ featuring an amidoalkene unit, which forms a weak chelate by orienting its double bond proximal to magnesium, is thermodynamically favourable relative to $C3$ with a mono-hapto N-ligated amidoalkene unit. This energy gap almost van-

ishes for mono-substrate-adducted species $C3' \cdot S$ and $C3 \cdot S$, which are virtually identical energetically. It is worth noting that species $C3'' \cdot S$, featuring η^1-amidoalkene/η^2-aminoalkene units are found less favourable thermodynamically than $C3' \cdot S$ (Figure S3 in the Supporting Information). With a further saturation of the coordinative sphere around magnesium by a second associated amine molecule, the tendency to form $C3' \cdot (S)^2$ decreases rapidly. All attempts to locate $C3' \cdot (S)^2$ with an intact (κ^3-ONN)Mg ligation were unsuccessful and only species featuring an (κ^2-ONN)Mg ligation with an substrate (NH)-stabilised dissociated NMe$_2$ arm could be located, which is moreover placed well above $C3 \cdot (S)^2$, with an intact (κ^3-ONN)Mg ligation, in energy.

As revealed from Figure 10, DFT predicts that the catalytically competent [{ONN}Mg(NHR)] compound is predominantly present as mono-substrate ($C3 \cdot S$, $C3' \cdot S$) adducted species, together with a less populated bis-amine adduct $C3 \cdot (S)^2$, all of which are expected to participate in rapid amine association/dissociation equilibria.[21]

The σ-insertive mechanism

Migratory olefin 1,2-insertion into the Mg–N amido σ-bond

Several imaginable trajectories for insertive cyclisation featuring an axial or equatorial approach of the olefin unit that start from $C3'$ or its mono- ($C3' \cdot S$) and bis-substrate ($C3' \cdot (S)^2$) adducted species have been examined. With regard to $C3' \cdot S$ and $C3' \cdot (S)^2$ precursor species, two families of trajectories are conceivable, which sees the Mg–N amido σ-bond being *trans* ($C3a' \cdot (S)^n \rightarrow C4a \cdot (S)^n$, Scheme 6) or *cis* ($C3b' \cdot (S)^n \rightarrow C4b \cdot (S)^n$, Scheme 7) disposed relative to the phenoxy group.[22]

Common to all the trajectories studied is that N–C bond formation evolves through a four-centre TS structure describing a metal-mediated migratory olefin insertion into the Mg–N amido σ-bond, which occurs at distances of approximately 2 Å for the emerging N–C bond. Following the reaction path fur-
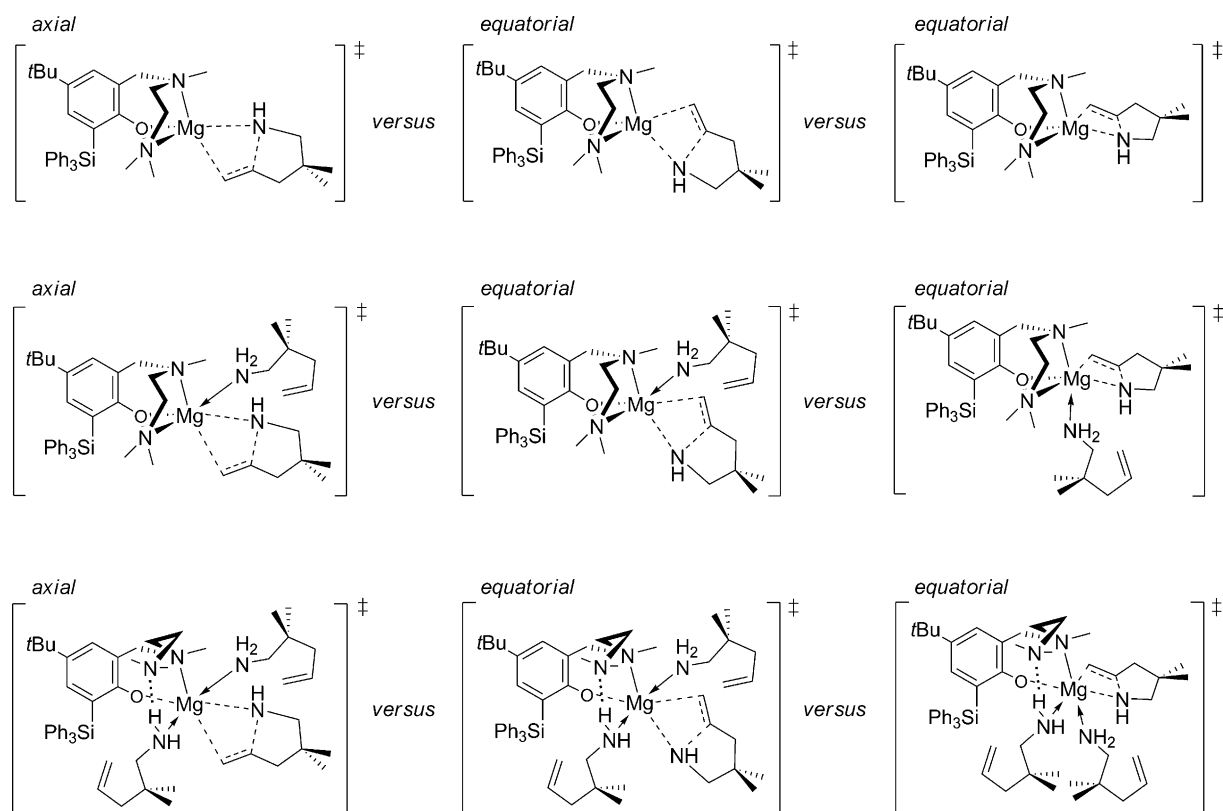
Scheme 6. Alternative trajectories for migratory olefin insertion into the Mg—N amido σ-bond at **C3′** (top) and its substrate adducted species **C3a′·S** (middle) and **C3a′·(S)²** (bottom), to involve substrate adducted species where amido is *trans* to the phenoxy group.
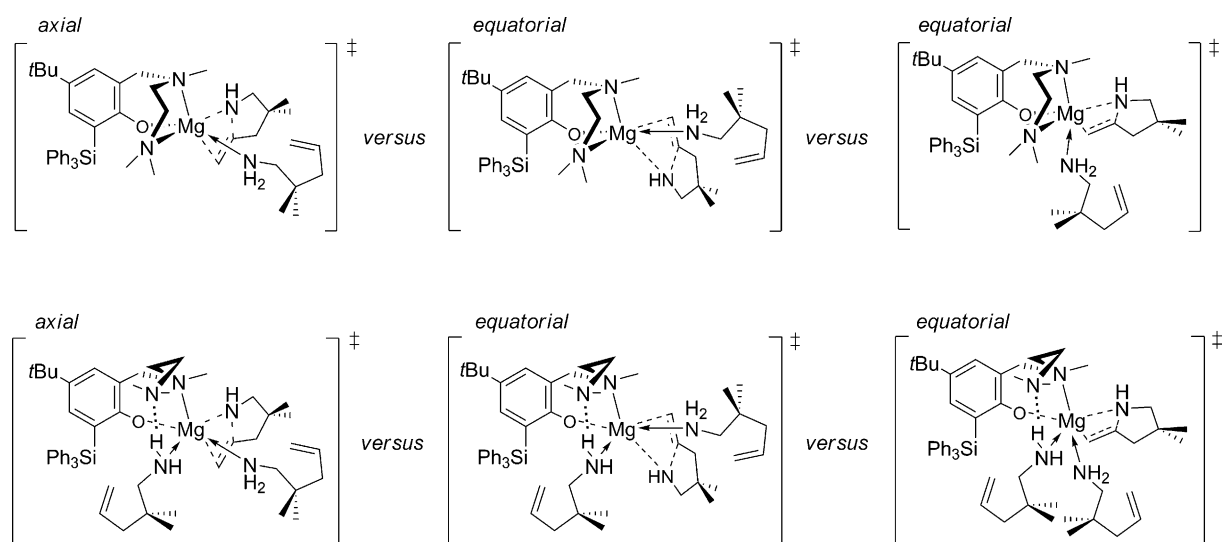
Scheme 7. Alternative trajectories for migratory olefin insertion into the Mg—N amido σ-bond at substrate adducted species **C3b′·S** (top) and **C3b′·(S)²** (bottom), to involve substrate adducted species where amido is *cis* to the phenoxy group.

ther, TS structures decay into {ONN}Mg alkyl intermediate **C4** (or **B** in Scheme 1), which has the azacycle bound to magnesium through its methylene tether and the N donor centre.

The condensed energy profiles in Figure 11 (exemplified for substrate adducted species featuring amido *cis* to the phenoxy group) reveal that substrate-free and mono-substrate-adduct-

ed {ONN}Mg species **C3′** and **C3′·S** are similarly competent at effecting insertive cyclisation, whilst enhanced steric pressure around the Mg centre through association of another substrate molecule renders migratory olefin insertion at **C3′·(S)²** substantially less favourable on both thermodynamic and kinetic grounds. Increased steric pressure along **C3′·(S)²→C4·(S)²** path-

ways is a direct consequence of the necessity of activating the olefin unit towards N—C bond formation by close contact with the electropositive metal centre and is manifested in the fact that species participating via **C3**′·(S)^2→**C4**·(S)^2 all feature a {κ^2-ONN}Mg ligation with an substrate(NH)-stabilised dissociated NMe$_2$ arm. Irrespective of whether one or two spectator substrate molecules are involved or whether the Mg—N amido σ-bond is *trans* (**C3a**′(S)^n→**C4a**(S)^n) or *cis* (**C3b**′(S)^n→**C4b**(S)^n) disposed relative to the phenoxy group, an equatorial approach of the olefin unit onto the Mg—N bond is found most favourable.[22]

Migratory olefin insertion following an equatorial trajectory preferably proceeds into the Mg—N amido σ-bond that is *trans* to the phenoxy unit and favours **C3a**′·S→**C4a**·S slightly over **C3**′→**C4**. The energetically prevalent **C3a**′·S→**C4a**·S insertive cyclisation has a modest barrier of 15.1 kcal mol^{-1} (relative to the prevalent **C3a$_1$**′·S form of the {ONN}Mg amido complex) to overcome and is endergonic (Figure S4a4 in the Supporting Information). For precursor species **C3b**′·(S)^n, which have amido and phenoxy groups *cis* disposed, olefin insertion is likely proceeding through **C3b**′·S→**C4b**·S, but is slightly more demanding kinetically ($\Delta G^{\ddagger} = 16.8$ kcal mol^{-1}, Figure 11, relative to the prevalent **C3a$_1$**′·S form of the {ONN}Mg amido complex). Hence, both **C3a**′·S→**C4a**·S and **C3b**′·S→**C4b**·S are likely traversed as most accessible pathways, although the latter with a somewhat smaller probability. All this characterises insertive ring closure for a sterically moderately encumbered {ONN}Mg amido catalyst species as a kinetically facile, reversible step that favours **C3**′·S. We note that a previous computational study[20] on cyclohydroamination of aminoalkene S by a tris(oxazolinyl)borate magnesium amido catalyst also revealed a kinetically modest and reversible insertion step with a barrier of similar magnitude ($\Delta G^{\ddagger} = 16.8$ kcal mol^{-1}),[20] but without the involvement of spectator amine molecules.

Mg—C azacycle tether aminolysis

The {ONN}Mg alkyl intermediate formed via the most accessible **C3a**′·S→**C4a**·S and **C3b**′·S→**C4b**·S pathways already has one substrate molecule complexed at magnesium, which is moreover favourably placed *cis* to the Mg—C linkage. Several trajectories for intramolecular H transfer have been probed for species generated via **C3a**·(S)^n→**C4a**·(S)^n (Scheme 8) and
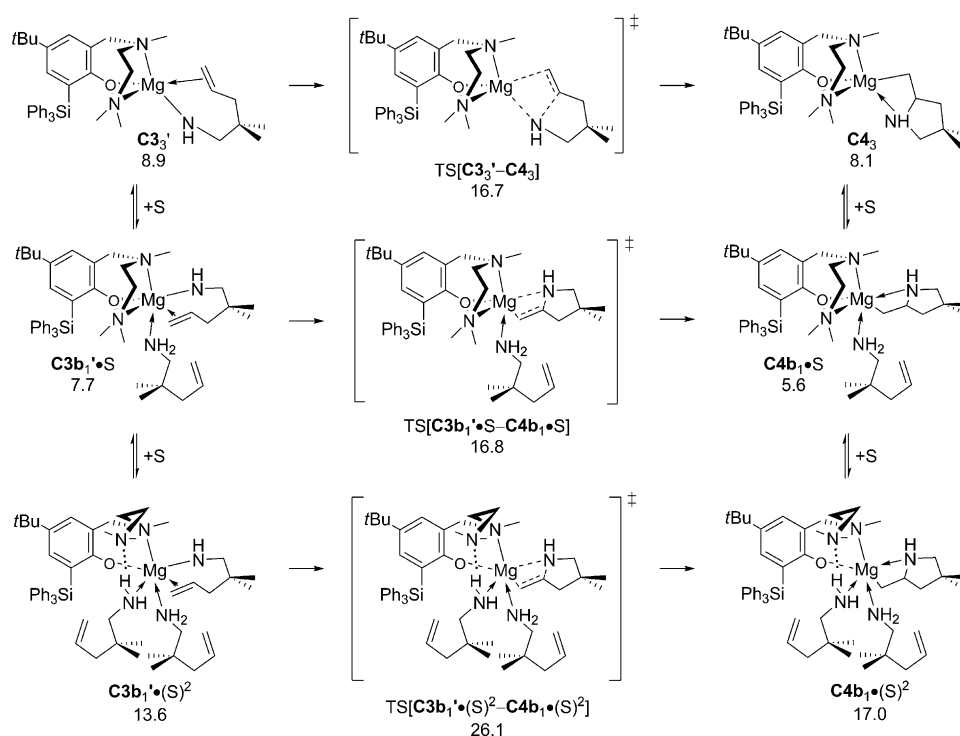
Figure 11. Most accessible pathways for migratory olefin insertion into the Mg Mg—N amido σ-bond at **C3**′ and its substrate adducted species **C3b**′·S and **C3b**′·(S)^2 to involve substrate adducted species featuring amido *cis* to the phenoxy unit.[23]

C3b·(S)^n→**C4b**·(S)^n (Scheme 9) pathways for insertive cyclisation.[22]

Aminolysis evolves through a metathesis-type TS structure that describes the cleavage of an already suitably polarised N—H bond and concurrent C—H bond formation. The process to commence at **C4a**·S, **C4b**·S involves species with an intact {κ^3-ONN}Mg ligation. In contrast, for intramolecular H transfer to occur at bis-amine adducts **C4a**·(S)^2, **C4b**·(S)^2, featuring an substrate N—H stabilised dissociated NMe$_2$ arm, a {κ^2-ONN}Mg ligation is maintained throughout. It places pathways with two substrate molecules participating at a higher energy than pathways with a single substrate molecule involved (Figure 12). Hence, excess substrate is unlikely facilitating Mg—C bond aminolysis on either thermodynamic or kinetic grounds.

Interestingly, **C4a**·S, **C4b**·S generated via preferably traversed pathways for insertive cyclisation to follow an equatorial trajectory are precursor species for the most accessible **C4a**·S→**C5** and **C4b**·S→**C5** pathways. Thus, neither association of another substrate molecule or substantial relaxation within the ligand sphere is required for protonolytic Mg—C bond cleavage to occur at the {ONN}Mg alkyl intermediate. The two **C4a**·S→**C5** and **C4b**·S→**C5** pathways have an identical intrinsic barrier (relative to its direct precursors **C4a**·S, **C4b**·S, respectively), but the stability gap between **C4a**·S and **C4b**·S, in favour of the latter, renders **C4b**·S→**C5** the most accessible pathway for Mg—C alkyl bond aminolysis (Figure 12, Figure S5a1 and Figure S5a3 in the Supporting Information). It features an intrinsic barrier of 11.9 kcal mol^{-1} (Figure 12, relative to **C4b**·S) and affords [{ONN}Mg(NHR)·(NHRR)] compound
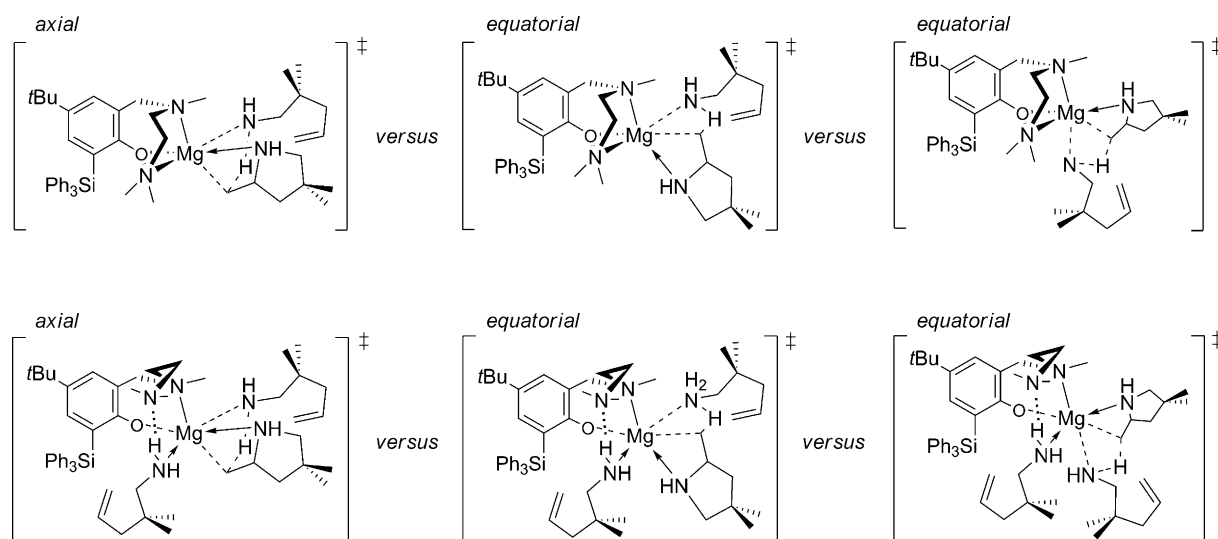
Scheme 8. Alternative trajectories for Mg—C azacycle tether aminolysis at the magnesium alkyl intermediate, which is generated via **C3 a**·(S)^n→**C4 a**·(S)^n, through pathways with one (top) or two (bottom) adducted substrate molecules involved.
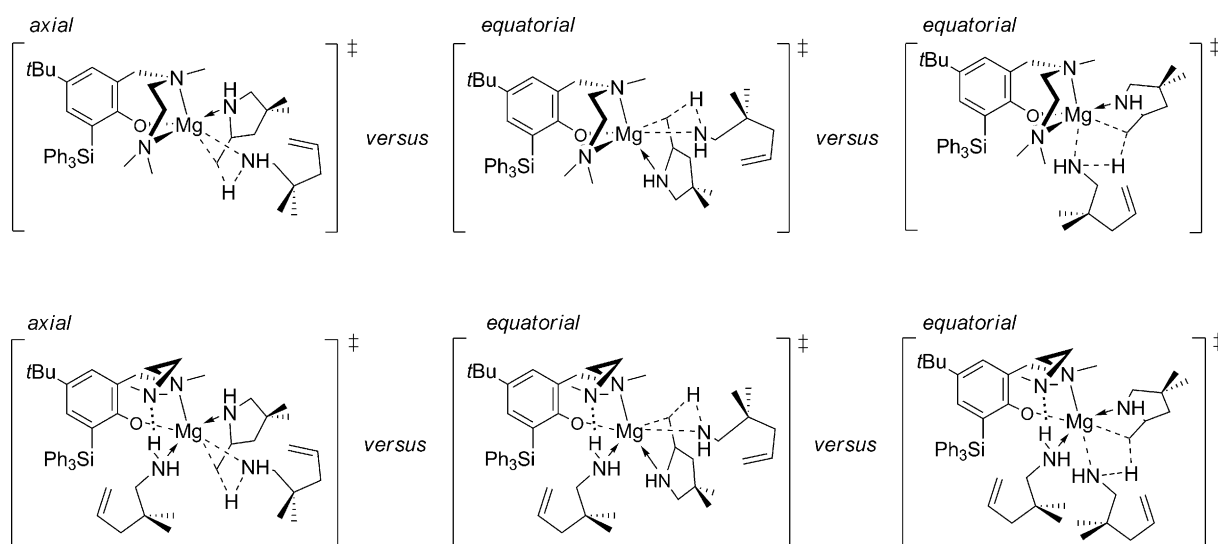
Scheme 9. Alternative trajectories for Mg—C azacycle tether aminolysis at the magnesium alkyl intermediate, which is generated via **C3 b**·(S)^n→**C4 b**·(S)^n, through pathways with one (top) or two (bottom) adducted substrate molecules involved.

C5 in a process that is downhill by 8.3 kcal mol^{-1} (relative to **C4 b**·S). The initially formed isomer **C5**$_1$ with an axially bound amido group is readily transformed thereafter into a thermo-dynamically more favourable isomer **C5**$_3$ featuring an equatorial amido.[22] The facile displacement of pyrrolidine P by substrate S at **C5** renders aminolysis even more favourable thermodynamically. The DFT predicted gap of 3.6 kcal mol^{-1} ($\Delta\Delta G^{\ddagger}$, Figure 12, Figure S5a1 and Figure S5a3 in the Supporting Information) between most accessible trajectories via **C4 a**·S→**C5** and **C4 b**·S→**C5** makes the former almost impossible to be traversed.

Overall, the DFT-derived smooth energy profile shown in Figure 12 is indicative of a kinetically affordable and exergonic, hence (together with subsequent downhill product displacement) irreversible, intramolecular Mg—C alkyl bond protonoly-

sis step via the most accessible **C4 b**·S→**C5** pathway. Participation of another coordinated amine molecule, however, is un-likely to facilitate the process on either thermodynamic or kin-etic grounds. It is worth nothing that the effective inaccess-ibility of rival **C4 a**·S→**C5** pathway has its primary origin in the stability gap between **C4 a**·S and **C4 b**·S, but not in their intrin-sic reactivity, which is of comparable magnitude.

Generation of a {ONN}Mg pyrrolide compound

A magnesium pyrrolide **C6**·(S)^n may represent a relevant off-cycle intermediate and could thus play a role in hydroamina-tion catalysis by the system at hands. Provided that the pyrro-lide is kinetically accessible at affordable costs, it could well compete with **C3**·(S)^n and **C5**·(S)^n for representing the catalyst
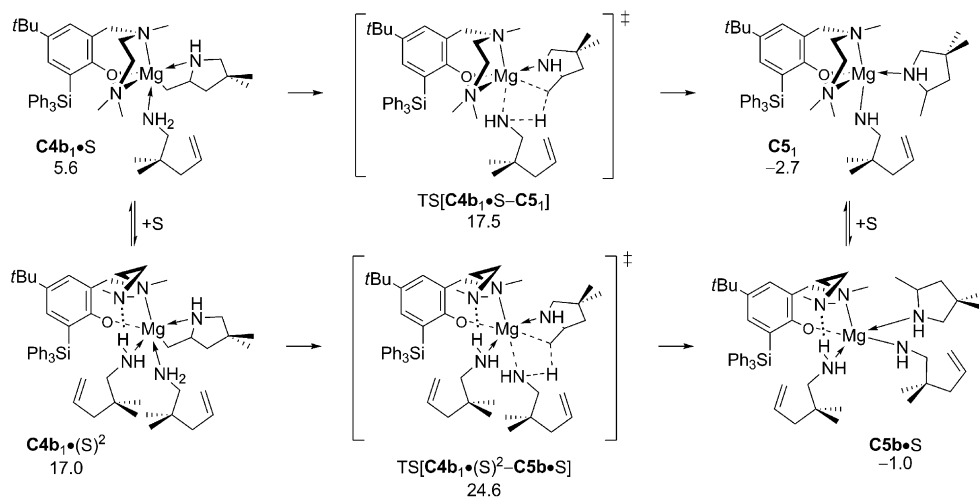
Figure 12. Most accessible pathways for Mg−C σ-bond aminolysis at amine-adducted species **C4 b**·S and **C4 b**·(S)^2 of the {ONN}Mg alkyl intermediate that are formed via **C3 b**·(S)^n→**C4 b**·(S)^n for insertive cyclisation.[23]

torial pyrrolide group is the prevalent form of the {ONN}Mg pyrrolide compound and bis-substrate adducted **C6**·(S)^2 and substrate-free **C6** species are at higher energy.[22]

The concerted proton-triggered cyclisation mechanism

The alternative mechanistic pathway outlined in Scheme 2, which describes N−C ring closure triggered by concomitant amino proton transfer onto the adjacent C=C linkage, thereby affording cycloamine products through a concerted single-step transformation, is studied next.

resting state. Noteworthy, a magnesium pyrrolide compound has been observed by NMR spectroscopy upon monitoring aminoalkene cyclisation by a tris(oxazolinyl)borate {To^M}Mg^{II} catalyst system.[12n]

To this end, plausible routes for generation of a {ONN}Mg pyrrolide have been examined, including: 1) intramolecular 1,3 H transfer at the Mg alkyl intermediate **C4**·(S)^n, a process that may benefit from participation of excess amine through a relay-type mechanism, and 2) cycloamine α-proton abstraction at intermediate **C5**·(S)^n. Similar to our findings for a related {To^M}Mg^{II} catalyst,[20] route B proves to be far more accessible when compared to route A and is likely the dominant pathways that leads to **C6**·(S)^n.

The energy profiles of the most accessible pathways to commence from **C5** and its mono-substrate adducted form, shown in Figure 13, reveal that α-proton abstraction preferably proceeds at **C5**, which is initially formed via the dominant **C4 b**·S→**C5** pathway for protonolytic Mg−C bond cleavage. The process is unlikely benefiting from complexation of another substrate molecule, thus paralleling the findings for the protonolysis step. Proton transfer evolves through a metathesis-type TS[**C5**−**C6**·S] with rather modest intrinsic barriers of 4.8 (**C5**→**C6**·S) and 15.5 kcal mol^{-1} (**C6**·S→**C5**) to afford substrate adducted {ONN}Mg pyrrolide **C6**·S in a process that is driven by a thermodynamic force of 10.7 kcal mol^{-1} (relative to **C5**). Thus, **C5**⇌**C6**·S conversion is kinetically feasible and reversible, but strongly favours **C6**·S. DFT predicts that **C6**·S with an equa-

Figure 13. Most accessible pathways for conversion of {ONN}Mg amido cycloamine compound **C5** into {ONN}Mg pyrrolide intermediate **C6**.[23]

The two trajectories examined involving N−C bond formation through an axial olefin approach at the Mg−N amido σ-bond, triggered by a proton transferred from an equatorially bound substrate, or alternatively describing concurrent ring closure at an equatorial Mg−N bond and proton delivery from an axially bound S (Scheme 10), are found to be equally viable, with the trajectory for axial olefin approach being somewhat preferred.[22]

The most accessible pathway following this trajectory starts with a facile conversion of the thermodynamically prevalent **C3 a**′·S into a conformer that has olefin and substrate moieties already favourably arranged and evolves through a six-centre TS structure that constitutes N−C^5 ring closure with concomitant transfer of a proton from a magnesium-bound and, hence, acidified substrate molecule on the adjacent olefin-C^6 centre. As exemplified in Figure 14 for the more accessible tra-
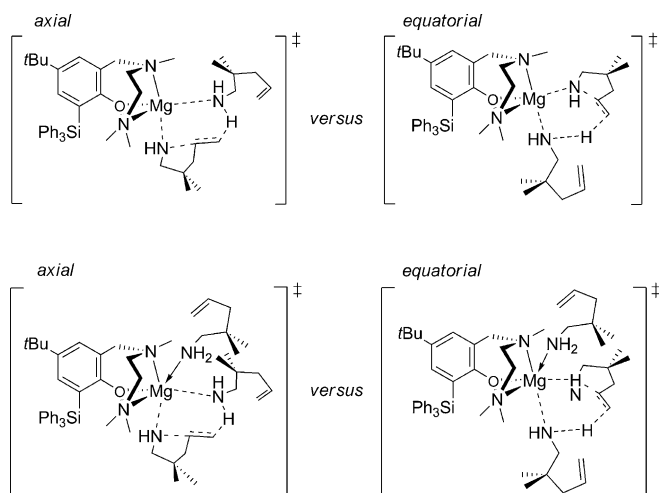
Scheme 10. Alternative trajectories for concerted proton-triggered N–C ring closure at **C3·S** (top) and **C3·(S)²** (bottom) adducts of the [{ONN}Mg(NHR)] complex.

Figure 14. Selected structural parameter [Å] of the optimised TS structure for proton-assisted concerted N–C/C–H bond formation at **C3 a′·S** via a trajectory for axial olefin approach.[24]

jectory of axial olefin approach, the located TS[**C3 a′·S–C5**] features a {κ³-ONN}Mg ligation with a N–C⁵ distance of 1.92 Å and vanishing N–H (1.17 Å) and emerging C–H (1.65 Å) bonds, which is indicative of a concerted, but asynchronous proton transfer. The rather large Mg–olefin distance (>3.6 Å) describes N–C ring closure occurring outside of the immediate vicinity of the alkaline earth, thereby reflecting that amino proton delivery activates the C= C linkage and not the close interaction with the electropositive metal as necessitated by the rival σ-insertive pathway. After passing through the TS structure, TS[**C3 a′·S–C5**] and TS[**C3·(S)²–C5 a·S**] decay into the {ONN}Mg amino cycloamine compound **C5** and its substrate adduct **C5 a·S**, respectively.

The dominant pathway for concurrent N–C ring closure and amino proton delivery at axial sites in **C3 a′·S** has a barrier of 23.1 kcal mol⁻¹ (relative to the prevalent **C3 a₁′·S** form of the {ONN}Mg amido complex) to overcome and affords **C5** in a process that is downhill by −6.3 kcal mol⁻¹ (Figure 15). Thus, proton-assisted concerted cyclisation is irreversible as is Mg–C alkyl bond aminolysis and both steps furnish compound **C5**. Similar to previous discussion for the aminolysis step, the association of another spectator substrate molecule does not serve stabilising product or TS structures and additional amine molecules are therefore unlikely to participate in this step (Figure 15). Noteworthy, TS[**C3·(S)²–C5 a·S**] still features an intact {κ³-ONN}Mg ligation whilst for protonolysis the participa-

Figure 15. Most accessible pathways for N–C bond formation with concurrent delivery of the amino proton to the olefin unit at the [{ONN}Mg(NHR)] compound with one (**C3·S**, top) or two (**C3·(S)²**, bottom) adducted substrate molecules.[23]

tion of an additional spectator substrate molecule provokes dissociation of an NMe₂ arm. This behaviour reflects the differences in spatial demands imposed at the metal centre whilst traversing σ-insertive and concerted proton-triggered mechanistic pathways.

Comparison of mechanistic pathways

Figure 16 collates the free-energy profiles assessed for alternative mechanistic scenarios for cyclohydroamination of *gem*-dimethyl-substituted aminoalkene S (**5 c**) to be mediated by phenoxyamine {ONN}Mg alkyl starting material **4 b** (R=SiPh₃). It focuses exclusively on the most accessible pathways to commence from the catalytically competent phenoxyamine
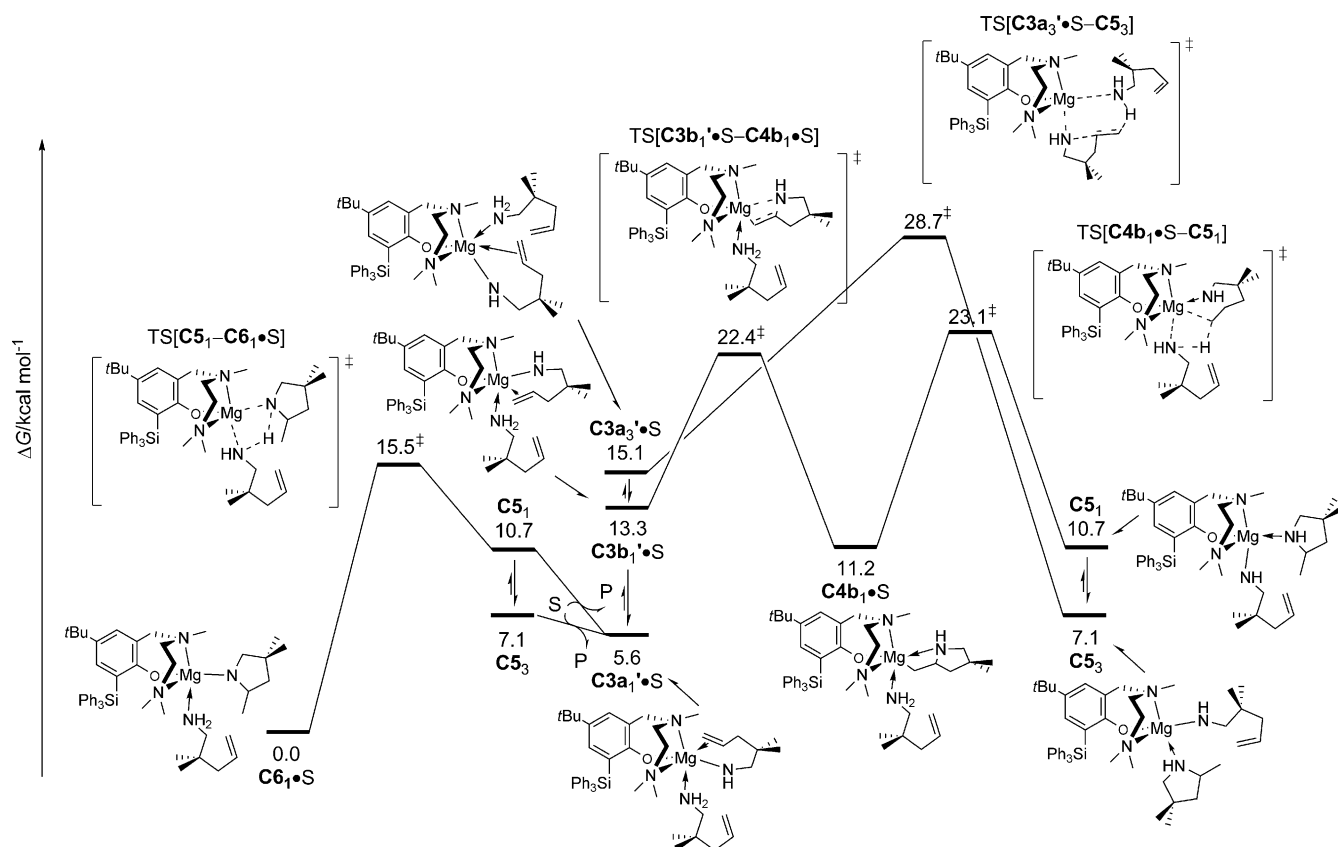
Figure 16. Condensed reaction profile for intramolecular hydroamination of *gem*-dimethyl-substituted aminoalkene **5c** (S) to be mediated by a phenoxyamine {ONN}Mg alkyl compound **4b** (R = SiPh$_3$) proceeding through alternative mechanistic cycles. Cycloamine product (P) liberation through **C5** + S → **C3a'·S** + P is included.[25]

[{ONN}Mg(NHR)] amido compound **C3**, which is readily generated through facile initial catalyst activation, whereas other less probable or energetically prohibitive pathways have been omitted. It is worth noting that the thermodynamic force for S → P cyclisation has been subtracted from **C5**, **C6·S** and TS[**C5**–**C6·S**].

It becomes clear from Figure 16 that substrate adducted {ONN}Mg pyrrolide **C6·S** is the most stable species associated to the catalytic cycle and thus likely corresponds to the catalyst resting state. It is readily converted into magnesium amido cycloamine compound **C5**; its most stable conformer **C5$_3$** is 7.1 kcal mol^{-1} higher in energy than **C6·S**. Subsequent displacement of cycloamine by amine substrate gives rise to the {ONN}Mg amido complex in a supposedly kinetically easy, downhill transformation. DFT predicts that the magnesium amido active catalyst complex **C3** is predominantly present as mono-substrate (**C3·S**, **C3'·S**) adducted species, the various possible conformers of which are expected to participate in rapid equilibria.[21]

The N–C ring closure with concurrent amino proton transfer taking place outside the immediate proximity of the electropositive magnesium centre via a six-centre TS[**C3a'·S**–**C5**] is (in combination with ensuing facile cycloamine displacement) irreversible[25a] and has a total barrier of 28.7 kcal mol^{-1} (relative to the catalyst resting state **C6·S**) to overcome. The observed large primary KIE is easily explained by this pathway, but the

σ-insertive pathways shown in Figure 16 is equally consistent. This pathway entails: 1) facile and reversible σ-insertive N–C bond forming cyclisation via **C3a'·S** → **C4a·S** or **C3b'·S** → **C4b·S** that favours the Mg amido catalyst species; 2) downhill turnover-limiting **C4b·S** → **C5** Mg–C σ-bond aminolysis at the {ONN}Mg alkyl intermediate; followed by 3) kinetically easy and exergonic displacement of cycloamine by substrate to regenerate the {ONN}Mg amido active catalyst complex.

The two mechanistic cycles account equally well for all the observed features of the process, are indistinguishable by an empirical rate law and are driven by a thermodynamic force of identical magnitude. DFT reveals that a proton-assisted concerted N–C/C–H bond forming pathway is energetically prohibitive in the presence of a kinetically less demanding σ-insertive pathway. The magnitude of the assessed kinetic disparity ($\Delta\Delta G^{\ddagger} = 5.6$ kcal mol^{-1}, Figure 16) is indicative that the σ-insertive pathway is likely traversed exclusively. The DFT predicted total barrier of 23.1 kcal mol^{-1} (relative to the catalyst resting state **C6·S**) for magnesium–alkyl bond aminolysis matches the experimentally determined Eyring parameter ($\Delta G^{\ddagger} = 24.1(\pm 0.6)$ kcal mol^{-1} (298 K)) gratifyingly well. DFT estimates a classical KIE of 2.7 (298 K) to be associated with turnover-limiting aminolysis via TS[**C4b$_3$·S**–**C5$_1$**].[32] Taking tunnelling into account,[32b] a primary KIE of 3.1 (298 K) was obtained, which is reasonably close[32d] to the observed value of 3.9 (vide supra).

Conclusion

In the quest to develop the mechanistic insight into the intramolecular hydroamination of aminoalkenes utilizing novel phenoxyamine magnesium compounds, a complementary synthetic and computational study has been conducted. For the well characterised cyclisation of *gem*-dimethyl-substituted aminoalkene **5 c** mediated by a phenoxyamine magnesium alkyl starting material **4 b**, a reliable DFT protocol (dispersion-corrected B97-D3 in conjunction with basis sets of triple-ζ quality and a sound treatment of bulk solvent effects) has been employed as an established and predictive means to scrutinise rival mechanistic pathways. Two plausible mechanistic scenarios are compatible with observed distinct process features, which include substantial primary KIEs and a second-order rate law. Firstly, a proton-triggered concerted N—C/C—H bond-forming mechanism, thereby accomplishing amidoalkene→cycloamine conversion in a single step and secondly, a stepwise σ-insertive pathway that involves rapid and reversible migratory olefin insertion into the Mg—N amido bond linked to irreversible and slower Mg—C alkyl bond aminolysis. The comprehensive computational examination discloses non-competitive kinetic demands for a pathway describing N—C ring closure taking place outside of the immediate proximity of the electropositive metal centre triggered by concurrent amino proton delivery at the C=C linkage evolving through a six-centre TS structure. It, thus, militates against the operation of a concerted non-insertive cyclisation pathway in the presence of a kinetically less demanding σ-insertive pathway. The magnitude of the assessed kinetic disparity indicated that the σ-insertive pathway is likely traversed exclusively. This pathway entails: 1) facile and reversible σ-insertive N—C bond forming cyclisation via **C3 a′·S**→**C4 a·S** or **C3 b′·S**→**C4 b·S** that favours the Mg amido catalyst species; 2) downhill turnover-limiting **C4 b·S**→**C5** Mg—C σ-bond aminolysis at the {ONN}Mg alkyl intermediate; followed by, 3) kinetically easy and exergonic displacement of cycloamine by substrate to regenerate the {ONN}Mg amido active catalyst complex. The DFT predicted effective barrier (relative to the {ONN}Mg pyrrolide resting state) for magnesium—alkyl bond aminolysis matches the empirically determined Eyring parameters gratifyingly well.

Taking all these aspects together, the mechanistic analysis by complementary experimental and computational approaches presented herein provides compelling evidence that aminoalkene hydroamination proceeds through a stepwise σ-insertive pathway in the presence of a catalytically competent phenoxyamine magnesium amido compound.

Experimental Section

General considerations

All operations were performed under an inert atmosphere of nitrogen or argon using standard Schlenk-line or glovebox techniques. Solvents and reagents were purified as stated previously.[13] Mg(CH$_2$Ph)$_2$(THF)$_2$[26] and 5-(*tert*-butyl)-2-hydroxy-3-(triphenylsilyl)-benzaldehyde,[27] 2,4-di-*tert*-butyl-6-(((2-(dimethylamino)ethyl)(me-

thyl)amino)methyl) (**3 a**)[28] and the aminoalkene substrates 2,2-diphenylpent-4-enyl amine (**5 a**),[3k] (1-allylcyclohexyl)methylamine (**5 b**),[8g] 2,2-dimethyl-pent-4-enyl amine (**5 c**),[29] (*E*)-2,2-dimethyl-5-phenylpent-4-en-1-amine (**5 d**),[4d] 2,2,5-triphenylpent-4-enyl amine (**5 e**),[30] 2,2-diphenylhex-5-enyl amine (**5 f**),[31] 1-(1-allylcyclohexyl)-*N*-benzylmethanamine (**5 g**)[8g] and *N*-allylpent-4-en-1-amine (**7**)[3e] were synthesized according to literature protocols. The hydroamination products 2-methyl-4,4-diphenylpyrrolidine (**6 a**),[3k] 3-methyl-2-azaspiro[4,5]decane (**6 b**),[3o] 2,4,4-trimethylpyrrolidine (**6 c**),[3c] 2-benzyl-4,4-dimethylpyrrolidine (**6 d**),[4d] 2-benzyl-4,4-diphenylpyrrolidine (**6 e**),[5l] 2-methyl-5,5-diphenylpiperidine (**6 f**),[3m] 2-benzyl-3-methyl-2-azaspiro[4.5]decane (**6 g**),[8g] and 1-allyl-2-methylpyrrolidine (**8**)[12f] are known compounds and were identified by comparison to the literature NMR spectroscopic data.

Synthesis and characterisation

Synthesis of 4-(*tert*-butyl)-2-(((2-(dimethylamino)ethyl)(methyl)-amino)methyl)-6-(triphenylsilyl)phenol (3 b): 5-(*tert*-Butyl)-2-hydroxy-3-(triphenylsilyl)benzaldehyde (872 mg, 2.0 mmol)[27] and *N,N,N′*-trimethylethylenediamine (612 mg, 6.0 mmol) were mixed in 1,2-dichloroethane (10 mL) and then treated with sodium triacetoxyborohydride (1.3 g, 6.0 mmol) and AcOH (360 mg, 6.0 mmol). The mixture was stirred at room temperature under a nitrogen atmosphere for 2 days. The reaction mixture was quenched by addition of aqueous saturated NaHCO$_3$ (100 mL), and the product was extracted with diethyl ether (3×50 mL). The combined organic layers were washed with water (3×100 mL) and dried over MgSO$_4$. The solvent was evaporated under vacuum to give the product as a white foam which was used without further purification. Yield: 845 mg (81%). ^{1}H NMR (500 MHz, CDCl$_3$): $\delta = 7.63$ (m, 6 H, Si(C$_6$*H*$_5$)$_3$), 7.36 (m, 9 H, Si(C$_6$*H*$_5$)$_3$), 7.05 (m, 2 H, aryl-H), 3.70 (s, 2 H, ArC*H*$_2$N), 2.55 (m, 2 H, NMeCH$_2$C*H*$_2$NMe$_2$), 2.38 (m, 2 H, NMeC*H*$_2$CH$_2$NMe$_2$), 2.31 (s, 3 H, NC*H*$_3$), 2.14 (s, 6 H, N(C*H*$_3$)$_2$), 1.11 ppm (s, 9 H, C(C*H*$_3$)$_3$); ^{13}C{^{1}H} NMR (125 MHz, CDCl$_3$): $\delta = 161.1$, 141.0, 136.6, 135.8, 134.7, 129.2, 128.4, 127.7, 120.9, 119.4 (aryl), 61.7 (ArCH$_2$), 57.1 (NMeCH$_2$CH$_2$NMe$_2$), 54.4 (NMeCH$_2$CH$_2$NMe$_2$), 45.6 (NMeCH$_2$CH$_2$N(CH$_3$)$_2$), 42.3 (N(CH$_3$)CH$_2$CH$_2$NMe$_2$), 34.1 (C(CH$_3$)$_3$), 31.7 ppm (C(CH$_3$)$_3$).

[(3 a)Mg(CH$_2$Ph)] (4 a): In the glovebox, an NMR tube was charged with **3 a** (16.0 mg, 0.05 mmol), Mg(CH$_2$Ph)$_2$(THF)$_2$ (17.5 mg, 0.05 mmol) and 0.6 mL of [D$_6$]benzene. Attempts to isolate complex **4 a** have failed so far, due to facile ligand redistribution processes during removal of solvent. Hence, complex **4 a** was prepared and used in situ for catalytic experiments. ^{1}H NMR (400 MHz, [D$_6$]benzene): $\delta = 7.62$ (d, $^4J_{H,H} = 3.0$ Hz, 1 H, aryl-H), 7.10 (m, 4 H, CH$_2$C$_6$*H*$_5$), 6.91 (d, $^4J_{H,H} = 3.0$ Hz, 1 H, aryl-H), 6.77 (m, 1 H, CH$_2$C$_6$*H*$_5$), 3.20 (d, $^2J_{H,H} = 12.0$ Hz, 1 H, ArC*H*$_2$N), 3.10 (d, $^2J_{H,H} = 12.0$ Hz, 1 H, ArC*H*$_2$N), 2.07 (m, 1 H, CH$_2$CH$_2$), 1.79 (s, 9 H, C(CH$_3$)$_3$, 2 H, CH$_2$C$_6$H$_5$), 1.74 (m, 3 H, NCH$_3$, m, 1 H, CH$_2$CH$_2$), 1.48 ppm (s, 9 H, C(CH$_3$)$_3$).

[(3 b)Mg(CH$_2$Ph)] (4 b): **3 b** (104 mg, 0.2 mmol) was dissolved in benzene (0.5 mL) and then Mg(CH$_2$Ph)$_2$(THF)$_2$ (70 mg, 0.2 mmol) was added. The reaction mixture was kept at room temperature for 5 min and then the solvent was removed under vacuum. The white residue was washed with hexanes (2×2 mL) at −50 °C and the product was collected and dried in vacuo for 1 h. Yield: 102 mg (80%). ^{1}H NMR (400 MHz, [D$_6$]benzene): $\delta = 8.02$ (m, 6 H, Si(C$_6$H$_5$)$_3$), 7.82 (d, $^4J_{H,H} = 2.8$ Hz, 1 H, aryl-H), 7.20 (m, 9 H, Si(C$_6$H$_5$)$_3$, 4 H, CH$_2$C$_6$H$_5$, 1 H aryl-H), 6.82 (m, 1 H, aryl-H), 3.62 (d, $^2J_{H,H} = 12.8$ Hz, 1 H, ArC*H*$_2$N), 2.55 (d, $^2J_{H,H} = 12.8$ Hz, 1 H, ArC*H*$_2$N), 2.24 (m, 1 H, CH$_2$CH$_2$), 1.71 (s, 2 H, CH$_2$C$_6$H$_5$), 1.62 (s, 3 H, NCH$_3$), 1.52 (m, 1 H, CH$_2$CH$_2$), 1.34 (s, 9 H, C(CH$_3$)$_3$), 1.30 (br, 6 H, N(CH$_3$)$_2$), 0.93 ppm (m, 2 H, CH$_2$CH$_2$); ^{13}C{^{1}H} NMR (125 MHz, [D$_6$]benzene): $\delta = 171.3$, 156.3,

137.9, 137.8, 137.0, 136.2, 131.0, 129.3, 129.0, 128.5, 124.8, 122.5, 121.4, 117.9 (aryl), 63.7 (ArCH_2N), 56.6 (NMeCH_2CH_2), 50.4 (NMeCH_2CH_2), 43.6 (NCH_3), 34.4 ($C(CH_3)_3$), 32.5 (C(CH_3)$_3$), 20.5 ppm ($CH_2C_6H_5$).

General procedure for NMR-scale catalytic hydroamination/cyclisation reactions

In the glovebox, a screw-cap NMR tube was charged with ferrocene (6.0 mg, 32.3 μmol), the catalyst (5.0 μmol) [D_6]benzene (0.6 mL), and the substrate (0.10 mmol). The NMR tube was sealed, removed from the glovebox and placed in the thermostated oil bath or thermostated ^{1}H NMR probe ($\pm 0.5\,^{\circ}$C) and the conversion was monitored by NMR spectroscopy by following the disappearance of the olefinic signals of the substrate relative to the internal standard ferrocene. NMR spectra were taken in appropriate time intervals (1.5 or 3 min). The error of measurement (shown as error bars in the raw kinetic plot) was estimated to $\pm 5\%$ based on the accuracy of integrating signals in a ^{1}H NMR spectrum. Errors on linear correlations were estimated from the standard error of the linear regression analysis performed using Microsoft Excel.

Computational details

All calculations based on Kohn–Sham density functional theory (DFT)[33] were performed by means of the program package TUR-BOMOLE[34] using the B97-D[35] generalized gradient approximation (GGA) functional within the RI-J integral approximation[36] in conjunction with flexible basis sets of triple-ζ quality. Empirical dispersion corrections by Grimme (D3 with Becke–Johnson damping)[37] were used to account for critical non-covalent interactions involved in the studied HA catalysis. For magnesium we used the (14s9p3d)/[5s5p3d] (def2-TZVPPD) all-electron basis set.[38] All remaining elements were represented by Ahlrich's valence triple-ζ def2-TZVPD basis set[38, 39a, b] with polarization functions on all atoms. The validity of the computational protocol employed for reliably mapping the energy landscape of alkaline-earth-mediated hydroamination has been substantiated before[18] and this allowed mechanistic conclusions with substantial predictive value to be drawn.

The free-energy landscape of the entire HA course was assessed for *gem*-dimethyl-substituted aminoalkene **5c** together with the phenoxyamine {ONN}Mg alkyl complex **4b** (R = SiPh$_3$) as starting material. No structural simplification of any of the key species involved was imposed. The DFT calculations have simulated the authentic reaction conditions by treating the bulk effects of the benzene solvent by a consistent continuum model in form of the conductor-like screening model for realistic solvents (COSMO-RS).[40] This solvation model includes continuum electrostatic and also solvent-cavitation and solute-solvent dispersion effects through surface-proportional terms. The free solvation enthalpy has been assessed with the aid of COSMO-RS at the BP86[41]/(def2-TZVPPD + def2-TZVPD)//BP86-D3/(def2-TZVPPD + def2-TZVPD)[38] level of approximation. Geometry optimisation and frequency calculations were performed at the B97-D3/(def2-TZVPPD + SV(P))[39c] level to confirm the nature of all optimised key structures and to determine thermodynamic parameters (298 K, 1 atm) under the conventional ideal-gas, rigid-rotor and quantum-mechanical harmonic-oscillator approximation. The entropy contributions for condensed-phase conditions were estimated based on computed gas-phase entropies by employing the procedure of Okuno.[42] The mechanistic conclusions drawn in this study were based on the Gibbs free-energy profile of the entire catalytic cycle assessed at the B97-D3(COSMO-RS)/(def2-TZVPPD + def2-TZVPD) level of approximation

for experimental condensed phase conditions. Calculated structures were visualised by employing the StrukEd program,[43] which was also used for the preparation of 3D molecule drawings.

[1] a) A. Ricci, *Modern Amination Methods*, Wiley-VCH, Weinheim, **2000**; b) A. Ricci, *Amino Group Chemistry: From Synthesis to the Life Sciences*, Wiley-VCH, Weinheim, **2008**.

[2] For reviews on hydroamination see: a) R. Taube, in *Applied Homogeneous Catalysis* (Eds.: B. Cornils, W. A. Herrmann), Wiley-VCH, Weinheim, **1996**, Vol. 1, p. 507; b) T. E. Müller, M. Beller, *Chem. Rev.* **1998**, *98*, 675; c) J. J. Brunet, D. Neibecker, in *Catalytic Heterofunctionalization from Hydroamination to Hydrozirconation* (Eds.: A. Togni, H. Grützmacher), Wiley-VCH, Weinheim, **2001**, p. 91; d) T. E. Müller, K. C. Hultzsch, M. Yus, F. Foubelo, M. Tada, *Chem. Rev.* **2008**, *108*, 3795; e) S. Doye, in *Science of Synthesis* (Ed: D. Enders), Thieme, Stuttgart, **2009**, Vol. 40a, p. 241; f) A. L. Reznichenko, K. C. Hultzsch, *Top. Organomet. Chem.* **2013**, *43*, 51; g) N. Nishina, Y. Yamamoto, *Top. Organomet. Chem.* **2013**, *43*, 115.

[3] Reviews on rare-earth metal-based catalysts: a) S. Hong, T. J. Marks, *Acc. Chem. Res.* **2004**, *37*, 673; b) A. L. Reznichenko, K. C. Hultzsch, *Struct. Bonding (Berlin)* **2010**, *137*, 1. For selected example of rare-earth metal-catalysed hydroaminations of aminoalkenes see: c) M. R. Gagne, C. L. Stern, T. J. Marks, *J. Am. Chem. Soc.* **1992**, *114*, 275; d) M. A. Giardello, V. P. Conticello, L. Brard, M. R. Gagné, T. J. Marks, *J. Am. Chem. Soc.* **1994**, *116*, 10241; e) Y. Li, T. J. Marks, *J. Am. Chem. Soc.* **1998**, *120*, 1757; f) Y. K. Kim, T. Livinghouse, J. E. Bercaw, *Tetrahedron Lett.* **2001**, *42*, 2933; g) Y. K. Kim, T. Livinghouse, *Angew. Chem. Int. Ed.* **2002**, *41*, 3645; *Angew. Chem.* **2002**, *114*, 3797; h) G. A. Molander, S. K. Pack, *Tetrahedron* **2003**, *59*, 10581; i) G. A. Molander, S. K. Pack, *J. Org. Chem.* **2003**, *68*, 9214; j) P. N. O'Shaughnessy, P. D. Knight, C. Morton, K. M. Gillespie, P. Scott, *Chem. Commun.* **2003**, 1770; k) S. Hong, S. Tian, M. V. Metz, T. J. Marks, *J. Am. Chem. Soc.* **2003**, *125*, 14768; l) J.-S. Ryu, T. J. Marks, F. E. McDonald, *J. Org. Chem.* **2004**, *69*, 1038; m) F. Lauterwasser, P. G. Hayes, S. Bräse, W. E. Piers, L. L. Schafer, *Organometallics* **2004**, *23*, 2234; n) K. C. Hultzsch, F. Hampel, T. Wagner, *Organometallics* **2004**, *23*, 2601; o) J. Y. Kim, T. Livinghouse, *Org. Lett.* **2005**, *7*, 1737; p) J. Collin, J.-D. Daran, O. Jacquet, E. Schulz, A. Trifonov, *Chem. Eur. J.* **2005**, *11*, 3455; q) E. Lu, W. Gan, Y. Chen, *Organometallics* **2009**, *28*, 2318; r) H. F. Yuen, T. J. Marks, *Organometallics* **2009**, *28*, 2423; s) T. K. Panda, C. G. Hrib, P. G. Jones, J. Jenter, P. W. Roesky, M. Tamm, *Eur. J. Inorg. Chem.* **2008**, 4270; t) L. J. E. Stanlake, L. L. Schafer, *Organometallics* **2009**, *28*, 3990; u) I. Aillaud, D. Lyubov, J. Collin, R. Guillot, J. Hannedouche, E. Schulz, A. Trifonov, *Organometallics* **2008**, *27*, 5929; v) D. V. Vitanova, F. Hampel, K. C. Hultzsch, *J. Organomet. Chem.* **2011**, *696*, 321; w) K. Manna, M. L. Kruse, A. D. Sadow, *ACS Catal.* **2011**, *1*, 1637; x) C. Queffelec, F. Boeda, A. Pouilhés, A. Meddour, C. Kouklovsky, J. Hannedouche, J. Collin, E. Schulz, *ChemCatChem* **2011**, *3*, 122; y) Y. Chapurina, H. Ibrahim, R. Guillot, E. Kolodziej, J. Collin, A. Trifonov, E. Schulz, J. Hannedouche, *J. Org. Chem.* **2011**, *76*, 10163; z) N. K. Hangaly, A. R. Petrov, K. A. Rufanov, K. Harms, M. Elfferding, J. Sundermeyer, *Organometallics* **2011**, *30*, 4544; aa) P. Benndorf, J. Kratsch, L. Hartenstein, C. M. Preuss, P. W. Roesky, *Chem. Eur. J.* **2012**, *18*, 14454.

[4] For biphenolate and binaphtholate rare-earth metal hydroamination catalysts see: a) D. V. Gribkov, K. C. Hultzsch, F. Hampel, *Chem. Eur. J.* **2003**, *9*, 4796; b) D. V. Gribkov, F. Hampel, K. C. Hultzsch, *Eur. J. Inorg. Chem.* **2004**, 4091; c) D. V. Gribkov, K. C. Hultzsch, *Chem. Commun.* **2004**, 730; d) D. V. Gribkov, K. C. Hultzsch, F. Hampel, *J. Am. Chem. Soc.* **2006**, *128*, 3748; e) A. L. Reznichenko, F. Hampel, K. C. Hultzsch, *Chem. Eur. J.* **2009**, *15*, 12819; f) A. L. Reznichenko, H. N. Nguyen, K. C. Hultzsch,

Angew. Chem. Int. Ed. **2010**, *49*, 8984; *Angew. Chem.* **2010**, *122*, 9168; g) A. L. Reznichenko, K. C. Hultzsch, *Organometallics* **2013**, *32*, 1394; h) X. Yu, T. J. Marks, *Organometallics* **2007**, *26*, 365.

[5] Reviews on Group 4 metal-based catalysts: a) F. Pohlki, S. Doye, *Chem. Soc. Rev.* **2003**, *32*, 104; b) I. Bytschkov, S. Doye, *Eur. J. Org. Chem.* **2003**, 935; c) S. Doye, *Synlett* **2004**, 1653; d) A. L. Odom, *Dalton Trans.* **2005**, 225; e) R. Severin, S. Doye, *Chem. Soc. Rev.* **2007**, *36*, 1407; f) P. Eisenberger, L. L. Schafer, *Pure Appl. Chem.* **2010**, *82*, 1503. For selected examples of hydroamination of aminoalkenes catalysed by Group 4 metals see: g) P. D. Knight, I. Munslow, P. N. O'Shaughnessy, P. Scott, *Chem. Commun.* **2004**, 894; h) D. V. Gribkov, K. C. Hultzsch, *Angew. Chem. Int. Ed.* **2004**, *43*, 5542; *Angew. Chem.* **2004**, *116*, 5659; i) J. A. Bexrud, J. D. Beard, D. C. Leitch, L. L. Schafer, *Org. Lett.* **2005**, *7*, 1959; j) H. Kim, P. H. Lee, T. Livinghouse, *Chem. Commun.* **2005**, 5205; k) D. A. Watson, M. Chiu, R. G. Bergman, *Organometallics* **2006**, *25*, 4731; l) C. Müller, C. Loos, N. Schulenberg, S. Doye, *Eur. J. Org. Chem.* **2006**, 2499; m) M. C. Wood, D. C. Leitch, C. S. Yeung, J. A. Kozak, L. L. Schafer, *Angew. Chem. Int. Ed.* **2007**, *46*, 354; *Angew. Chem.* **2007**, *119*, 358; n) A. L. Gott, A. J. Clarke, G. J. Clarkson, P. Scott, *Organometallics* **2007**, *26*, 1729; o) B. D. Stubbert, T. J. Marks, *J. Am. Chem. Soc.* **2007**, *129*, 6149; p) C. Müller, R. Koch, S. Doye, *Chem. Eur. J.* **2008**, *14*, 10430; q) C. Müller, W. Saak, S. Doye, *Eur. J. Org. Chem.* **2008**, 2731; r) S. Majumder, A. L. Odom, *Organometallics* **2008**, *27*, 1174; s) A. L. Reznichenko, K. C. Hultzsch, *Organometallics* **2010**, *29*, 24; t) L. E. N. Allan, G. J. Clarkson, D. J. Fox, A. L. Gott, P. Scott, *J. Am. Chem. Soc.* **2010**, *132*, 15308; u) D. C. Leitch, R. H. Platel, L. L. Schafer, *J. Am. Chem. Soc.* **2011**, *133*, 15453; v) K. Manna, W. C. Everett, G. Schoendorff, A. Ellern, T. L. Windus, A. D. Sadow, *J. Am. Chem. Soc.* **2013**, *135*, 7235; w) E. Chong, S. Qayyum, L. L. Schafer, R. Kempe, *Organometallics* **2013**, *32*, 1858.

[6] Group 5 metal catalysts: a) A. L. Reznichenko, T. J. Emge, S. Audörsch, E. G. Klauber, K. C. Hultzsch, B. Schmidt, *Organometallics* **2011**, *30*, 921; b) F. Zhang, H. Song, G. Zi, *Dalton Trans.* **2011**, *40*, 1547.

[7] Review on actinide-based catalysts: a) T. Andrea, M. S. Eisen, *Chem. Soc. Rev.* **2008**, *37*, 550. For selected examples of actinide-catalysed hydroamination of aminoalkenes, see: b) B. D. Stubbert, T. J. Marks, *J. Am. Chem. Soc.* **2007**, *129*, 4253; c) E. M. Broderick, N. P. Gutzwiller, P. L. Diaconescu, *Organometallics* **2010**, *29*, 3242; d) C. E. Hayes, R. H. Platel, L. L. Schafer, D. B. Leznoff, *Organometallics* **2012**, *31*, 6732. See also ref. [5o].

[8] Reviews on late transition metal-based catalysts: a) M. Beller, C. Breindl, M. Eichberger, C. G. Hartung, J. Seayad, O. R. Thiel, A. Tillack, H. Trauthwein, *Synlett* **2002**, 1579; b) J. F. Hartwig, *Pure Appl. Chem.* **2004**, *76*, 507; c) R. A. Widenhoefer, X. Han, *Eur. J. Org. Chem.* **2006**, 4555; d) J. J. Brunet, N. C. Chu, M. Rodriguez-Zubiri, *Eur. J. Inorg. Chem.* **2007**, 4711; e) K. D. Hesp, M. Stradiotto, *ChemCatChem* **2010**, *2*, 1192; f) J. Jenter, A. Lühl, P. W. Roesky, S. Blechert, *J. Organomet. Chem.* **2010**, *695*, 406. Selected recent examples: for the hydroamination of non-activated alkenes: g) C. F. Bender, R. A. Widenhoefer, *J. Am. Chem. Soc.* **2005**, *127*, 1070; h) A. Zulys, M. Dochnahl, D. Hollmann, K. Löhnwitz, J.-S. Herrmann, P. W. Roesky, S. Blechert, *Angew. Chem. Int. Ed.* **2005**, *44*, 7794; *Angew. Chem.* **2005**, *117*, 7972; i) X. Han, R. A. Widenhoefer, *Angew. Chem. Int. Ed.* **2006**, *45*, 1747; *Angew. Chem.* **2006**, *118*, 1779; j) F. E. Michael, B. M. Cochran, *J. Am. Chem. Soc.* **2006**, *128*, 4246; k) C. Liu, J. F. Hartwig, *J. Am. Chem. Soc.* **2008**, *130*, 1570; l) C. F. Bender, W. B. Hudson, R. A. Widenhoefer, *Organometallics* **2008**, *27*, 2356; m) E. B. Bauer, G. T. S. Andavan, T. K. Hollis, R. J. Rubio, J. Cho, G. R. Kuchenbeiser, T. R. Helgert, C. S. Letko, F. S. Tham, *Org. Lett.* **2008**, *10*, 1175; n) J.-W. Pissarek, D. Schlesiger, P. W. Roesky, S. Blechert, *Adv. Synth. Catal.* **2009**, *351*, 2081; o) Z. Zhang, S. D. Lee, R. A. Widenhoefer, *J. Am. Chem. Soc.* **2009**, *131*, 5372; p) X. Shen, S. L. Buchwald, *Angew. Chem. Int. Ed.* **2010**, *49*, 564; *Angew. Chem.* **2010**, *122*, 574; q) K. D. Hesp, S. Tobisch, M. Stradiotto, *J. Am. Chem. Soc.* **2010**, *132*, 413; r) L. D. Julian, J. F. Hartwig, *J. Am. Chem. Soc.* **2010**, *132*, 13813; s) Z. Liu, H. Yamamichi, S. T. Madrahimov, J. F. Hartwig, *J. Am. Chem. Soc.* **2011**, *133*, 2772; t) C. S. Sevov, J. Zhou, J. F. Hartwig, *J. Am. Chem. Soc.* **2012**, *134*, 11960; u) M. Rodriguez-Zubiri, C. Baudequin, A. Béthegnies, J.-J. Brunet, *ChemPlusChem* **2012**, *77*, 445; v) E. Bernoud, P. Oulié, R. Guillot, M. Mellah, J. Hannedouche, *Angew. Chem. Int. Ed.* **2014**, *53*, 4930; *Angew. Chem.* **2014**, *126*, 5030.

[9] a) J. Seayad, A. Tillack, C. G. Hartung, M. Beller, *Adv. Synth. Catal.* **2002**, *344*, 795; b) R. D. Closson, J. P. Napolitano, G. G. Ecke, A. Kolka, *J. Org. Chem.* **1957**, *22*, 646; c) B. W. Howk, E. L. Little, S. L. Scott, G. M. Whit-

man, *J. Am. Chem. Soc.* **1954**, *76*, 1899; d) R. Wegler, G. Pieper, *Chem. Ber.* **1950**, *83*, 1.

[10] For selected examples of hydroamination of alkenes catalysed by alkali metals see: a) M. Beller, C. Breindl, T. H. Riermeier, M. Eichberger, H. Trauthwein, *Angew. Chem. Int. Ed.* **1998**, *37*, 3389; *Angew. Chem.* **1998**, *110*, 3571; b) D. Tzalis, C. Koradin, P. Knochel, *Tetrahedron Lett.* **1999**, *40*, 6193; c) A. Ates, C. Quinet, *Eur. J. Org. Chem.* **2003**, 1623; d) V. Khedkar, A. Tillack, C. Benisch, J.-P. Melder, M. Beller, *J. Mol. Catal. A* **2005**, *241*, 175; e) P. Horrillo Martínez, K. C. Hultzsch, F. Hampel, *Chem. Commun.* **2006**, 2221; f) T. Ogata, A. Ujihara, S. Tsuchida, T. Shimizu, A. Kaneshige, K. Tomioka, *Tetrahedron Lett.* **2007**, *48*, 6648; g) C. Quinet, P. Jourdain, C. Hermans, A. Ates, I. Lucas, I. E. Markó, *Tetrahedron* **2008**, *64*, 1077; h) J. Deschamp, J. Collin, J. Hannedouche, E. Schulz, *Eur. J. Org. Chem.* **2011**, 3329.

[11] Reviews on the application of alkaline-earth metal catalysts: a) S. Harder, *Chem. Rev.* **2010**, *110*, 3852; b) A. G. M. Barrett, M. R. Crimmin, M. S. Hill, P. A. Procopiou, *Proc. R. Soc. London Ser. A* **2010**, *466*, 927; c) M. R. Crimmin, M. S. Hill, *Top. Organomet. Chem.* **2013**, *45*, 191; d) S. Kobayashi, Y. Yamashita, *Acc. Chem. Res.* **2011**, *44*, 58.

[12] For examples of alkaline-earth metal-based hydroamination catalysts see: a) M. R. Crimmin, I. J. Casely, M. S. Hill, *J. Am. Chem. Soc.* **2005**, *127*, 2042; b) S. Datta, P. W. Roesky, S. Blechert, *Organometallics* **2007**, *26*, 4392; c) S. Datta, M. T. Gamer, P. W. Roesky, *Organometallics* **2008**, *27*, 1207; d) A. G. M. Barrett, M. R. Crimmin, M. S. Hill, P. B. Hitchcock, G. Kociok-Köhn, P. A. Procopiou, *Inorg. Chem.* **2008**, *47*, 7366; e) F. Buch, S. Harder, *Z. Naturforsch. B* **2008**, *63*, 169; f) M. R. Crimmin, M. Arrowsmith, A. G. M. Barrett, I. J. Casely, M. S. Hill, P. A. Procopiou, *J. Am. Chem. Soc.* **2009**, *131*, 9670; g) A. G. M. Barrett, C. Brinkmann, M. R. Crimmin, M. S. Hill, P. Hunt, P. A. Procopiou, *J. Am. Chem. Soc.* **2009**, *131*, 12906; h) M. Arrowsmith, M. S. Hill, G. Kociok-Köhn, *Organometallics* **2009**, *28*, 1730; i) M. Arrowsmith, A. Heath, M. S. Hill, P. B. Hitchcock, G. Kociok-Köhn, *Organometallics* **2009**, *28*, 4550; j) P. Horrillo-Martínez, K. C. Hultzsch, *Tetrahedron Lett.* **2009**, *50*, 2054; k) M. Arrowsmith, M. S. Hill, G. Kociok-Köhn, *Organometallics* **2011**, *30*, 1291; l) J. Jenter, R. Köppe, P. W. Roesky, *Organometallics* **2011**, *30*, 1404; m) M. Arrowsmith, M. R. Crimmin, A. G. M. Barrett, M. S. Hill, G. Kociok-Köhn, P. A. Procopiou, *Organometallics* **2011**, *30*, 1493; n) J. F. Dunne, D. B. Fulton, A. Ellern, A. D. Sadow, *J. Am. Chem. Soc.* **2010**, *132*, 17680; o) A. Mukherjee, S. Nembenna, T. K. Sen, S. P. Sarish, P. K. Ghorai, H. Ott, D. Stalke, S. K. Mandal, H. W. Roesky, *Angew. Chem. Int. Ed.* **2011**, *50*, 3968; *Angew. Chem.* **2011**, *123*, 4054; p) S. R. Neal, A. Ellern, A. D. Sadow, *J. Organomet. Chem.* **2011**, *696*, 228; q) J. S. Wixey, B. D. Ward, *Chem. Commun.* **2011**, *47*, 5449; r) J. S. Wixey, B. D. Ward, *Dalton Trans.* **2011**, *40*, 7693; s) T. D. Nixon, B. D. Ward, *Chem. Commun.* **2012**, *48*, 11790; t) C. Brinkmann, A. G. M. Barrett, M. S. Hill, P. A. Procopiou, *J. Am. Chem. Soc.* **2012**, *134*, 2193; u) B. Liu, T. Roisnel, J.-F. Carpentier, Y. Sarazin, *Angew. Chem. Int. Ed.* **2012**, *51*, 4943; *Angew. Chem.* **2012**, *124*, 5027; v) B. Liu, T. Roisnel, J.-F. Carpentier, Y. Sarazin, *Chem. Eur. J.* **2013**, *19*, 2784; w) B. Liu, T. Roisnel, J.-F. Carpentier, Y. Sarazin, *Chem. Eur. J.* **2013**, *19*, 13445.

[13] a) X. Zhang, T. J. Emge, K. C. Hultzsch, *Organometallics* **2010**, *29*, 5871; b) X. Zhang, T. J. Emge, K. C. Hultzsch, *Angew. Chem. Int. Ed.* **2012**, *51*, 394; *Angew. Chem.* **2012**, *124*, 406.

[14] D. Seyferth, *Organometallics* **2009**, *28*, 1598.

[15] a) P. W. Roesky, T. E. Müller, *Angew. Chem. Int. Ed.* **2003**, *42*, 2708; *Angew. Chem.* **2003**, *115*, 2812; b) K. C. Hultzsch, *Adv. Synth. Catal.* **2005**, *347*, 367; c) K. C. Hultzsch, *Org. Biomol. Chem.* **2005**, *3*, 1819; d) I. Aillaud, J. Collin, J. Hannedouche, E. Schulz, *Dalton Trans.* **2007**, 5105; e) G. Zi, *Dalton Trans.* **2009**, 9101; f) A. L. Reznichenko, K. C. Hultzsch, in *Chiral Amine Synthesis: Methods, Developments and Applications* (Ed: T. Nugent), Wiley-VCH, Weinheim, **2010**, p.341; g) G. Zi, *J. Organomet. Chem.* **2011**, *696*, 68; h) J. Hannedouche, J. Collin, A. Trifonov, E. Schulz, *J. Organomet. Chem.* **2011**, *696*, 255; i) A. L. Reznichenko, A. J. Nawara-Hultzsch, K. C. Hultzsch, *Top. Curr. Chem.* **2014**, *343*, 191.

[16] For studies on the application of phenoxyamine alkaline-earth complexes as initiators in the polymerization of cyclic esters and lactide, see: a) J. Ejfler, M. Kobyłka, L. B. Jerzykiewicz, P. Sobota, *Dalton Trans.* **2005**, 2047; b) Y. Sarazin, R. H. Howard, D. L. Hughes, S. M. Humphrey, M. Bochmann, *Dalton Trans.* **2006**, 340; c) D. J. Darensbourg, W. Choi, C. P. Richers, *Macromolecules* **2007**, *40*, 3521; d) Z. Zheng, G. Zhao, R. Fablet, M. Bouyahyi, C. M. Thomas, T. Roisnel, O. Casagrande, Jr., J.-F. Carpentier, *New J. Chem.* **2008**, *32*, 2279; e) M. G. Davidson, C. T. O'Hara,

M. D. Jones, C. G. Keir, M. F. Mahon, G. Kociok-Köhn, *Inorg. Chem.* **2007**, *46*, 7686; f) V. Poirier, T. Roisnel, J.-F. Carpentier, Y. Sarazin, *Dalton Trans.* **2009**, 9820; g) W.-C. Hung, C.-C. Lin, *Inorg. Chem.* **2009**, *48*, 728; h) J. Ejfler, K. Krauzy-Dziedzic, S. Szafert, L. B. Jerzykiewicz, P. Sobota, *Eur. J. Inorg. Chem.* **2010**, 3602; i) Y. Sarazin, V. Poirier, T. Roisnel, J.-F. Carpentier, *Eur. J. Inorg. Chem.* **2010**, 3423; j) B. Liu, T. Roisnel, J.-P. Guégan, J.-F. Carpentier, Y. Sarazin, V. Poirier, T. Roisnel, J.-F. Carpentier, *Chem. Eur. J.* **2012**, *18*, 6289.

[17] The synthesis and X-ray structural analysis of complex **1 a** is reported in: A. R. F. Cox, V. C. Gibson, E. L. Marshall, A. J. P. White, D. Yeldon, *Dalton Trans.* **2006**, 5014.

[18] For DFT studies on the rare-earth metal-catalysed hydroamination, see: a) A. Motta, G. Lanza, I. L. Fragalà, T. J. Marks, *Organometallics* **2004**, *23*, 4097; b) A. Motta, I. L. Fragalà, T. J. Marks, *Organometallics* **2006**, *25*, 5533; c) S. Tobisch, *J. Am. Chem. Soc.* **2005**, *127*, 11979; d) S. Tobisch, *Chem. Eur. J.* **2005**, *11*, 6372; e) S. Tobisch, *Chem. Eur. J.* **2006**, *12*, 2520; f) S. Tobisch, *Chem. Eur. J.* **2007**, *13*, 9127; g) S. Tobisch, *Chem. Eur. J.* **2010**, *16*, 13814; h) S. Tobisch, *Dalton Trans.* **2012**, *41*, 9182; i) S. Tobisch, *Chem. Eur. J.* **2014**, *20*, 8988.

[19] S. Tobisch, *Inorg. Chem.* **2012**, *51*, 3786.

[20] S. Tobisch, *Chem. Eur. J.* **2011**, *17*, 14974.

[21] Substrate association and dissociation at the various intermediates is presumably facile and rapid equilibria are expected; examination by a linear-transit approach gave no indication that such processes are associated with a significant enthalpic barrier.

[22] See the Supporting Information for more detail.

[23] The prevalent [{ONN}Mg(NHR)·(NH₂R)] form **C3 a**₁′·S, featuring a chelating amidoalkene unit, of the competent catalyst complex (with the appropriate number of substrate S or cycloamine P molecules) has been chosen as reference for relative free energies (given in kcal mol^{-1}).

[24] The *t*Bu, SiPh₃ and methyl groups of the phenoxyamine {ONN}Mg ligand backbone are in grey together with a truncated display of the aminoalkene in order to enhance the visualisation of crucial structural aspects.

[25] Please note that the thermodynamic force of 7.8 kcal mol^{-1} for S→P cyclisation has been subtracted from **C5**, TS[**C5**–**C6**·S] and **C6**·S in Figure 16; The most stable conformer of **C5** and **C6**·S is included in Figure 16.

[26] R. R. Schrock, *J. Organomet. Chem.* **1976**, *122*, 209.

[27] A. N. Thadani, Y. Huang, V. H. Rawal, *Org. Lett.* **2007**, *9*, 3873.

[28] C. K. Williams, L. E. Breyfogle, S. K. Choi, W. Nam, J. Victor, G. Young, M. A. Hillmyer, W. B. Tolman, *J. Am. Chem. Soc.* **2003**, *125*, 11350.

[29] Y. Tamaru, M. Hojo, H. Higashimura, Z. Yoshida, *J. Am. Chem. Soc.* **1988**, *110*, 3994.

[30] D. S. C. Black, J. E. Doyle, *Austr. J. Chem.* **1978**, *31*, 2247.

[31] T. Kondo, T. Okada, T. Mitsudo, *J. Am. Chem. Soc.* **2002**, *124*, 186.

[32] The primary KIE has been estimated from the deviation of zero-point vibrational energies and partition function values for S and [D₂]-S substrates. Zero curvature tunnelling has been accounted for by the Skodje and Truhlar approximation, see: a) R. T. Skodje, D. G. Truhlar, B. C. Garrett, *J. Phys. Chem.* **1981**, *85*, 3019; the accuracy of computationally predicted k_H/k_D values for hydrogen transfer processes is limited by transition-state theory approximation, semi-classical tunnelling corrections and rigid rotator, harmonic oscillator approximation for vibrational frequencies, see: b) D. H. Lu, D. Maurice, D. G. Truhlar, *J. Am. Chem. Soc.* **1990**, *112*, 6206.

[33] R. G. Parr, W. Yang, *Density-Functional Theory of Atoms and Molecules*, Oxford University Press, Oxford, **1989**.

[34] a) R. Ahlrichs, M. Bär, M. Häser, H. Horn, C. Kölmel, *Chem. Phys. Lett.* **1989**, *162*, 165; b) O. Treutler, R. Ahlrichs, *J. Chem. Phys.* **1995**, *102*, 346; c) R. Ahlrichs, F. Furche, C. Hättig, W. Klopper, M. Sierka, F. Weigend, TURBOMOLE, version 6.0, University of Karlsruhe, **2009**, http://www.turbomole.com.

[35] a) S. Grimme, *J. Comput. Chem.* **2006**, *27*, 1787; b) A. D. Becke, *J. Chem. Phys.* **1997**, *107*, 8554.

[36] a) O. Vahtras, J. Almlöf, M. W. Feyereisen, *Chem. Phys. Lett.* **1993**, *213*, 514; b) K. Eichkorn, O. Treutler, H. Öhm, M. Häser, R. Ahlrichs, *Chem. Phys. Lett.* **1995**, *242*, 652.

[37] a) S. Grimme, J. Anthony, S. Ehrlich, H. Krieg, *J. Chem. Phys.* **2010**, *132*, 154104; b) S. Grimme, S. Ehrlich, L. Goerigk, *J. Comput. Chem.* **2011**, *32*, 1456; c) http://toc.uni-muenster.de/DFTD3/getd3.html.

[38] a) F. Weigend, R. Ahlrichs, *Phys. Chem. Chem. Phys.* **2005**, *7*, 3297; b) F. Weigend, *Phys. Chem. Chem. Phys.* **2006**, *8*, 1057.

[39] a) A. Schäfer, C. Huber, R. Ahlrichs, *J. Chem. Phys.* **1994**, *100*, 5829; b) K. Eichkorn, F. Weigend, O. Treutler, R. Ahlrichs, *Theor. Chem. Acc.* **1997**, *97*, 119; c) A. Schäfer, C. Huber, R. Ahlrichs, *J. Chem. Phys.* **1992**, *97*, 2571.

[40] a) A. Klamt, G. Schüürmann, *J. Chem. Soc. Perkin Trans. 2* **1993**, 799; b) A. Klamt, *J. Phys. Chem.* **1995**, *99*, 2224; c) F. Eckert, A. Klamt, *AIChE J.* **2002**, *48*, 369.

[41] a) A. D. Becke, *Phys. Rev. A* **1988**, *38*, 3098; b) J. P. Perdew, *Phys. Rev. B* **1986**, *33*, 8822.

[42] Y. Okuno, *Chem. Eur. J.* **1997**, *3*, 212.

[43] For further details, see http://www.struked.de.